

THE UNIVERSITY OF MICHIGAN
COLLEGE OF ENGINEERING
Department of Mechanical Engineering

Progress Report
For the period January 1, 1966 to March 31, 1966

DIESEL ENGINE IGNITION AND COMBUSTION

Jay A. Bolt
N. A. Henein

ORA Project 06720

under contract with:

U. S. ARMY
DETROIT PROCUREMENT DISTRICT
CONTRACT NO. DA-20-018-AMC-1669T
DETROIT, MICHIGAN

administered through:

OFFICE OF RESEARCH ADMINISTRATION ANN ARBOR

May 1966

enqn

UMR 0425

no. 1

TABLE OF CONTENTS

	Page
LIST OF FIGURES	v
NOMENCLATURE AND SYMBOLS	vii
INTRODUCTION	1
IGNITION DELAY—DEFINITIONS	3
REVIEW OF PREVIOUS WORK	4
Wolfer's Formula	4
Bauer's Formula	4
West's Formula	5
Rosen's Formula	5
Tsao, Myers, and Uyehara	5
EXPERIMENTAL WORK	
A. Crank Position for Maximum Pressure in a Motored Engine	8
B. Effect of Fuel-Air Ratio on Ignition Lag	10
C. Effect of Injection Pressure on Ignition Delay	12
D. Effect of Surface Temperature on Ignition Delay	15
E. Effect of Turbulence on Ignition Delay	15
COMPUTATIONS	
A. Gas Temperature	26
B. Rate of Heat Release	26
C. Index of Compression and Expansion	29
D. Rate of Fuel Injection	31
E. Combustion Computations	31
CONCLUSIONS	35
RECOMMENDATIONS	36
APPENDIX I: INSTRUMENTATION IMPROVEMENT	37
A. Pressure-Rise Delay	37
B. Illumination Delay	41
APPENDIX II: TEST CONDITIONS AND RESULTS	43
A. Test Conditions	43
B. Results	43

TABLE OF CONTENTS (Continued)

	Page
APPENDIX III: HEAT RELEASE	44
BIBLIGRAPHY	45

LIST OF FIGURES

Figure		Page
1	Ignition lag vs. $T_c \log P_c$ by West.	6
2	Maximum pressure advance in motored Lister Blackstone engine ($N = 980$ rpm, coolant temperature = 104.5°F).	9
3	Effect of fuel-air ratio on ignition delay, and injection advance.	11
4	Effect of fuel-air ratio on B.S.F.C. and I.S.F.C.	13
5	Effect of injector opening pressure on ignition delay.	14
6	Effect of injector opening pressure on I.S.F.C.	16
7	Effect of cooling water temperature on ignition delay.	17
8	Effect of cooling water temperature on injection start.	18
9	Turbulence in modified combustion chamber of Lister engine.	19
10	Air speed in the tangential passage to the swirl chamber of Lister engine at 1000 rpm.	20
11	Effect of engine speed on illumination delay.	22
12	Effect of engine speed on pressure-rise delay.	23
13	Effect of engine speed on I.S.F.C.	24
14	Effect of engine speed on injection advance.	25
15	Gas pressure and temperature during the cycle.	27
16	Rate of heat release and accumulated heat release diagrams.	28
17	P-V relationship on a Log-Log sheet.	30
18A	Nozzle needle assembly.	32
18B	Area for fuel flow vs. needle lift.	32

LIST OF FIGURES (Continued)

Figure		Page
19	Rate of fuel injection and accumulated fuel diagrams.	33
20	Pressure and pressure differentiating circuits.	38
21A	Pressure trace.	39
21B	Pressure differential trace.	39
22	Lag between the pressure and the pressure differentiating circuits.	40
23	Visicorder traces.	42

NOMENCLATURE AND SYMBOLS

- a = constant
- A = area of cylinder bore, in.²
- A_f = area of flow for fuel, in.²
- b = constant for each fuel
- C = constant for each fuel
- c_d = coefficient of discharge
- c_p = specific heat at constant pressure, $\frac{\text{BTu}}{\text{lbm } ^\circ\text{F}}$
- c_v = specific heat at constant volume, $\frac{\text{BTu}}{\text{lbm } ^\circ\text{F}}$
- D = diameter, in.
- g = gravitational acceleration, ft/sec²
- I.D. = ignition delay in milliseconds if not otherwise stated
- J = mechanical equivalent of heat, $\frac{\text{ft lbf}}{\text{BTu}}$
- K = ratio of specific heats
- k_a = thermal conductivity for air, $\frac{\text{BTu}}{\text{ft}^2 \text{ } ^\circ\text{F}/\text{ft.}}$
- m = mass, lb
- n = constant, or index of a polytropic process
- N = revolutions per minute
- P = gas pressure, psia
- P_a = air gauge pressure before flow meter
- P_b = barometric pressure, in. Hg
- P_c = compression pressure at start of injection, psia, or atm
- P_f = fuel pressure, psia

Q = quantity of heat, Btu
 r_f = radius of fuel droplet, ft
 R = universal gas constant, $\frac{\text{lb}_f \text{ ft}}{\text{lbm } ^\circ\text{R}}$
 t_c = chemical ignition delay, sec
 T_a = air temperature before air flow meter, $^\circ\text{F}$
 T_c = compression temperature at start of injection, $^\circ\text{F}$, $^\circ\text{R}$, or $^\circ\text{K}$
 T_{ci} = cooling water temperature at inlet to engine, $^\circ\text{F}$
 T_{ce} = cooling water temperature at exit from engine, $^\circ\text{F}$
 $T_{exh.}$ = exhaust gas temperature, $^\circ\text{F}$
 T_f = temperature of fuel, $^\circ\text{F}$
 T_i = self ignition temperature of fuel, $^\circ\text{F}$
 U = internal energy
 V = volume
 W = work
 W_B = brake load on dynamometer, lb
 θ = crank angles, degree
 ζ_f = specific weight of fuel, lb/ft^3
 X = exponent

INTRODUCTION

The work which had been done in the period from January 1, 1966, to March 31, 1966, included both theoretical and experimental investigations of the combustion process in diesel engines. Some work has been done to study the possibility of improving the sensitivity of the instruments assembled on the Lister-Blackstone engine, as described in a previous report(2).*

The theoretical part deals with an analytical study of the process of combustion of hydrocarbons in general, with special emphasis on the environment that occurs in the diesel engine. This theoretical study verified that there are factors which can significantly affect the combustion process, other than the pressure and temperature of the air, and the type of fuel. Unfortunately these factors have not been emphasized or evaluated in most previous publications. These factors are:

1. the fuel-air ratio
2. the injection pressure
3. turbulence
4. wall temperatures

It was decided to study these factors and to run experiments to find out how much they affect the combustion process. This was done to establish a test procedure for future runs in which these factors will be held constant or nearly so.

Prior to the above investigation on the factors that affect the combustion process, an additional experimental study was carried out concerning the air pressure and temperature at the end of the compression stroke. This investigation started after comparing the pressure and crankangle traces and observing that, with the engine motored, the point of maximum pressure is in advance of the point of T.D.C. A thermodynamic analysis was then made for the air during the compression stroke, the results of which supported our conclusion that the heat loss from the air to the cylinder wall is the main reason for the pressure reaching a maximum before top dead center.

The study made for the possible improvement of the accuracy of the instrumentation was in the following areas:

1. the detection of the point of pressure rise due to combustion. This had been done by applying a differential circuit to the output signal of the cylinder pressure transducer.

* Numbers in parantheses refer to the Bibliography.

2. The simultaneous recording of all signals for the same cycle, by using a Minneapolis-Honeywell visicorder. This simultaneous method of recording eliminates the errors caused by cycle to cycle variations.
3. The detection of the start of illumination more accurately by using a photo multiplier instead of the solar cell.

A complete cycle analysis was made for a sample run and a computer program was written for the same run.

This report covers a review of the previous work done and the results of the experimental work and cycle analysis.

IGNITION DELAY—DEFINITIONS

Previous investigators used various definitions for the ignition delay, based on the criteria used to define the end of this delay period. Most of the investigators used the start of pressure rise resulting from combustion as the end of this period. Others used the start of temperature rise due to combustion, or illumination.

In this investigation, it was noted that the start of pressure rise and the start of illumination did not occur simultaneously, and it seemed logical to differentiate between the different delay periods. The start of the illumination can be considered to be the end of the preflame chemical reactions of the first fuel particles to ignite. The start of illumination probably does not coincide with measurable pressure increase due to combustion. At this stage of the work it was found useful to define the different delay periods as follows:

1. Physical delay: is defined as the period of time required for the physical changes to occur to the fuel from the liquid phase to the vapor phase. It can be considered equal to the period of time between the beginning of injection and the beginning of preflame reaction.
2. Chemical delay: is defined as the period from the end of the physical delay to the beginning of ignition. During this period preflame reactions are considered to occur.
3. Illumination delay: is the time that elapses between the beginning of injection and the start of illumination.
4. Pressure rise delay: is the time that elapses between the beginning of injection and a measurable pressure rise due to combustion.
5. Temperature rise delay: is the time that elapses between the beginning of injection and a measurable temperature rise due to combustion. Evidently the illumination, pressure rise, and temperature rise delays are different from the physical and chemical delays.

Most of the literature concerning diesel combustion utilizes the pressure rise delay, probably because it is the easiest to measure, and because it is the most important from an engineering viewpoint. The pressure rise delay is often referred to as being the sum of the physical and chemical delays. In view of the above definitions, it is believed that this is inaccurate. In this report the ignition delay will be given in terms of illumination and pressure rise delays.

REVIEW OF PREVIOUS WORK

Most of the reported work on ignition delay was in the form of experimental investigations in a constant volume bomb. Little work was done on an engine. Few formulae are available for the ignition delay, and most of them relate the delay with the air pressure and temperature only. The following is a brief review of the formulae available.

WOLFER'S FORMULA (9)

The relation between the chemical delay and pressure and temperature can be derived from chain reaction theory and is given by the following equation:

$$t_c = \frac{c e^{\frac{b}{T_c}}}{P_c^n} \quad (1)$$

This formula applies to a homogeneous gas-phase reaction.

Wolfer used this equation for diesel fuels in a spherical constant volume vessel, and evaluated the constants and obtained the following formula.

$$\text{I.D.} = \frac{0.44}{P_c^{1.19}} e^{\frac{(4650)}{T_c}} \quad (2)$$

where: I.D. is in seconds, T in degree Kelvin, and P in atmospheres. The vessel was so arranged that turbulence could be created by a rotating inner liner. However, no reference for turbulence was given in this formula.

BAUER'S FORMULA (3)

Bauer put forward a theory that ignition delay, to a first approximation, is a function of $T_c \log P_c$, where P_c is in atmospheres, and T_c is degrees Kelvin or

$$\text{I.D.} = f(T_c \log P_c) \quad (3)$$

The exact nature of this function was not stated, but it was noticed that the experimental results showed similar characteristics to Wolfer's experiments in the constant-volume vessel.

WEST'S FORMULA (8)

West measured the pressure rise delay by running tests on a single-cylinder, open chamber diesel engine, 4.5" x 5.75", C.R. = 15.8:1, at a speed of 1000 rpm, at intake pressures ranging from 30" Hg. to 56" Hg. The results of ignition delay were correlated in terms of $T_c \log P_c$ as suggested by Bauer and are shown in Figure 1.

ROSEN'S FORMULA

Rosen in the paper of Ref. 6 gave a formula to relate the ignition delay with fuel properties, droplet size and compression temperature as follows:

$$I.D. = \frac{1200 r_f^2 \zeta_f c_p}{k_a} \log_e \frac{T_c - T_f}{T_c - T_i} \quad (4)$$

TSAO, MYERS, AND UYEHARA

The experimental results of these workers, Ref. 7, for the delay period were obtained from tests carried out with a C.F.R. engine incorporating a modified piston. The end of the delay period was considered to be at the point at which rapid increase in temperature occurred. The "null method" of infrared temperature measurement was used, employing an optical pyrometer.

The formula given by the author's is an empirical relationship for ignition delay as a function of the temperature, pressure, and engine speed. The formula for temperature rise ignition delay is as follows:

$$I.D. = 1000 e^x - 1000 \quad (5)$$

where

$$x = \frac{1}{1000} \left(\frac{123}{P_c} + 0.415 \right) \left\{ \left(\frac{-36.3}{T_c} + 0.0222 \right) N + \left(\frac{47.45 \times 10^3}{T_c} - 26.66 \right) + \left(\frac{T_c}{1000} - 1.45 \right) \left(\frac{1000 - N}{60} \right) \right\} \quad (6)$$

where the pressures are in psia and temperatures in °R. This equation in the simplified form is as follows:

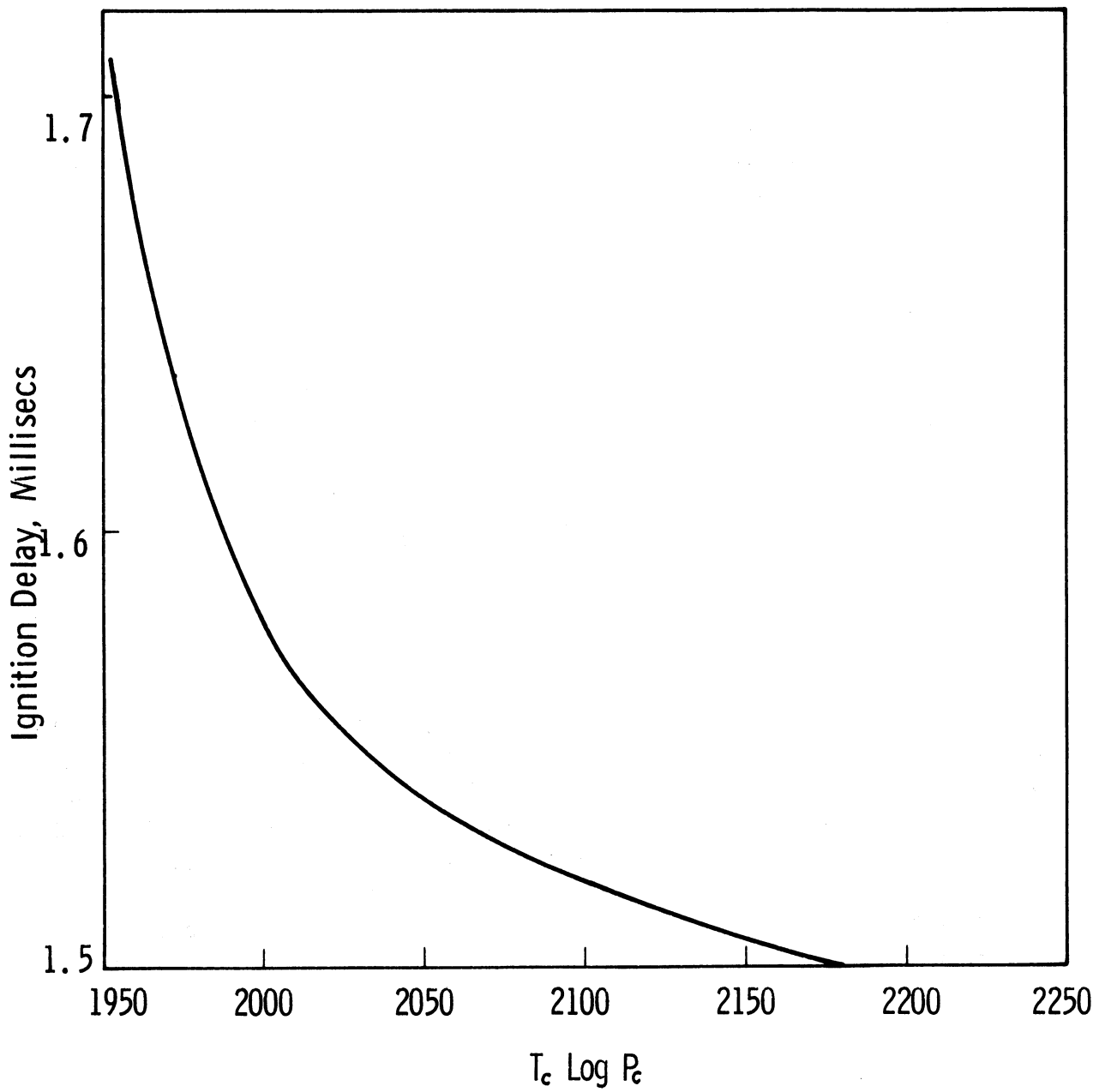


Figure 1. Ignition lag vs. $T_c \log P_c$ by West. (T_c in degrees Kelvin, P_c in psia).

$$\text{I.D.} = \left(\frac{123}{P_c} + 0.415 \right) \left\{ \left(\frac{-36.3}{T_c} + 0.0222 \right) N + \left(\frac{47.45 \times 10^3}{T_c} - 26.66 \right) + \left(\frac{T_c}{1000} - 1.45 \right) \left(\frac{1000 - N}{60} \right) \right\} \quad (7)$$

EXPERIMENTAL WORK

A. CRANK POSITION FOR MAXIMUM PRESSURE IN A MOTORED ENGINE

It has commonly been assumed that the maximum pressure occurs at T.D.C. in a motored engine and often the maximum pressure point has been used to determine the phase relationship. In our experimental data on the Lister engine it was noticed that the point of maximum pressure occurs in advance of the T.D.C. as shown in Figure 2. In this report the difference between the crank angle at which maximum pressure occurs, and the T.D.C., will be called the maximum pressure advance in a motored engine. After re-examining the accuracy of the making unit, which is set to determine the crank degrees on the scope screen, the engine was motored in the reverse direction. The pressure traces obtained indicated that maximum pressure also occurs, at almost the same point, before T.D.C. The difference between the maximum pressure advances in the two opposite directions is 0.2° of a crank angle. This is considered to be due to the change in heat losses caused by the change in valve timing when the engine was cranked in the opposite direction. This test indicated that the settings of the degree marking disc and pickup probe are correct.

A thermodynamic analysis was then made on the air during the compression stroke and the following formula was obtained for the pressure gradient at T.D.C.

$$\frac{dP}{d\theta} = \frac{R}{c_v} \cdot \frac{1}{V} \cdot \frac{dQ}{d\theta} \quad (8)$$

where

$$\frac{dQ}{d\theta} = \text{rate of heat transfer to the air with respect to crank angle degrees.}$$

At the end of the compression stroke the heat transfer $dQ/d\theta$ has a negative sign because heat is lost from the air to cylinder walls. Therefore $dQ/d\theta$ should have a negative sign indicating that the maximum pressure for a motored engine should occur before T.D.C.

This conclusion is also supported by published data of Tsao *et al.*, (Ref. 7), for the compression temperature in a diesel engine. The compression temperature was measured by applying the infrared null method. Figures 3, 5, and 9 of this reference indicate that the maximum temperature occurs before T.D.C. during the compression stroke. Accordingly the maximum pressure should also occur before T.D.C.

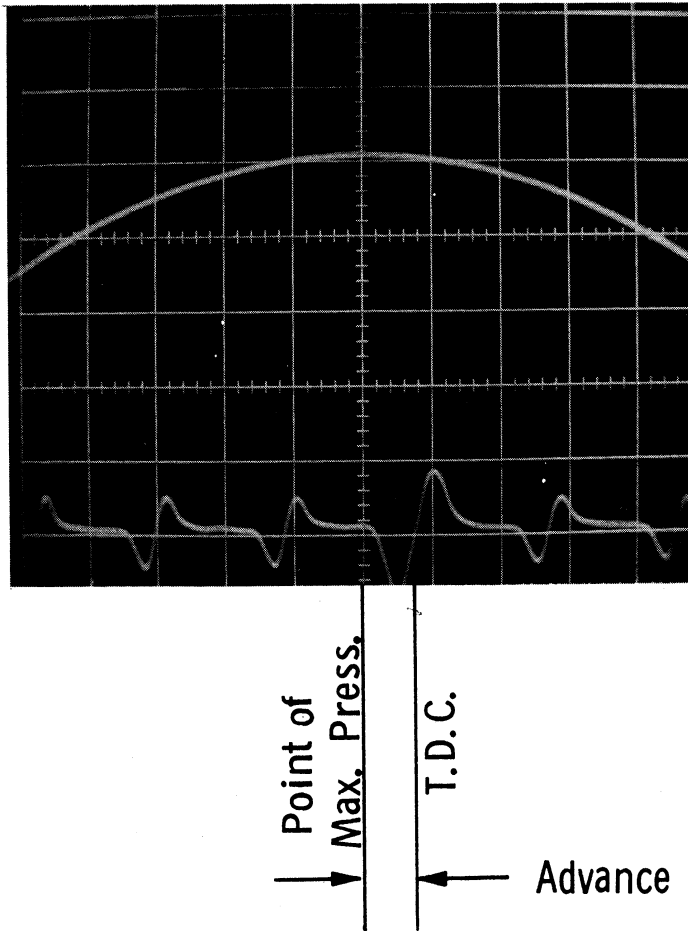


Figure 2. Maximum pressure advance in motored Lister Blackstone engine ($N = 980$ rpm, coolant temperature = 104.5°F).

This analysis indicated that the maximum pressure advance at the end of the compression stroke of a motored engine is mainly caused by the cooling losses. And, since the gas pressure and temperature at the end of compression in the engine affect the delay period, therefore the cooling losses should have an effect on delay period. This effect has been investigated and the results are given in Section D of this experimental work.

B. EFFECT OF FUEL-AIR RATIO ON IGNITION LAG

In a chemical process concentration of the reactants is an important factor that affects the rate of reaction. In the diesel engine, at the time of ignition there occur in the combustion chamber local fuel-air ratios ranging from zero to infinity. Ignition takes place in some region where the fuel-air ratio is optimum. This is generally in the envelope of the spray and is affected by many parameters such as type of fuel, its atomization, penetration and air turbulence. However, it is believed that if these factors are kept constant there exists some limits on the lean and rich sides beyond which the ignition will not occur or, at least, will be irregular. Starting with the lean limit, it is believed that an increase in fuel-air ratio would increase the probability of ignition start and the reaction speed and consequently reduce the ignition delay.

To find the effect of fuel-air ratio an ignition delay experiments were run at variable fuel-air ratios with the other parameters kept constant. On the lean side the engine was motored with fuel injection and combustion. The amount of fuel injected was reduced, and fuel-air ratios as low as 0.00216, (0.0325 stoichiometric), were reached. With the engine producing power the fuel-air ratio was increased up to 85% the stoichiometric ratio. With higher fuel-air ratios erratic operation of the engine occurred due to a very late after injection. By examining the cylinder pressure under these conditions it was noticed that ignition of the left-over fuel from the previous cycle occurred before the start of injection.

The results of this series of runs are plotted in Figures 3 and 4. Figure 3 indicates that the limit of irregular combustion on the lean side is at a fuel-air ratio of 0.0059 (0.089 - the stoichiometric ratio). The general trend of this figure indicates that the ignition delay decreases with the increase in fuel-air ratio. An increase in fuel-air ratio from .011 to 0.043 caused the illumination ignition delay to decrease by 32%. It should be noted that at higher fuel-air ratios, the solar cell did not operate properly. The decrease in pressure rise delay amounted to 34% by an increase in fuel-air ratio from 0.011 to 0.0568.

The effect of fuel-air ratio on decreasing the ignition lag is actually more than indicated in Figure 3, because at higher fuel-air ratios fuel injection starts at an earlier angle before T.D.C. i.e., at lower air pressures, temperatures, and densities. The advance in the start of fuel injection at different fuel-air ratios is shown also in Figure 3.

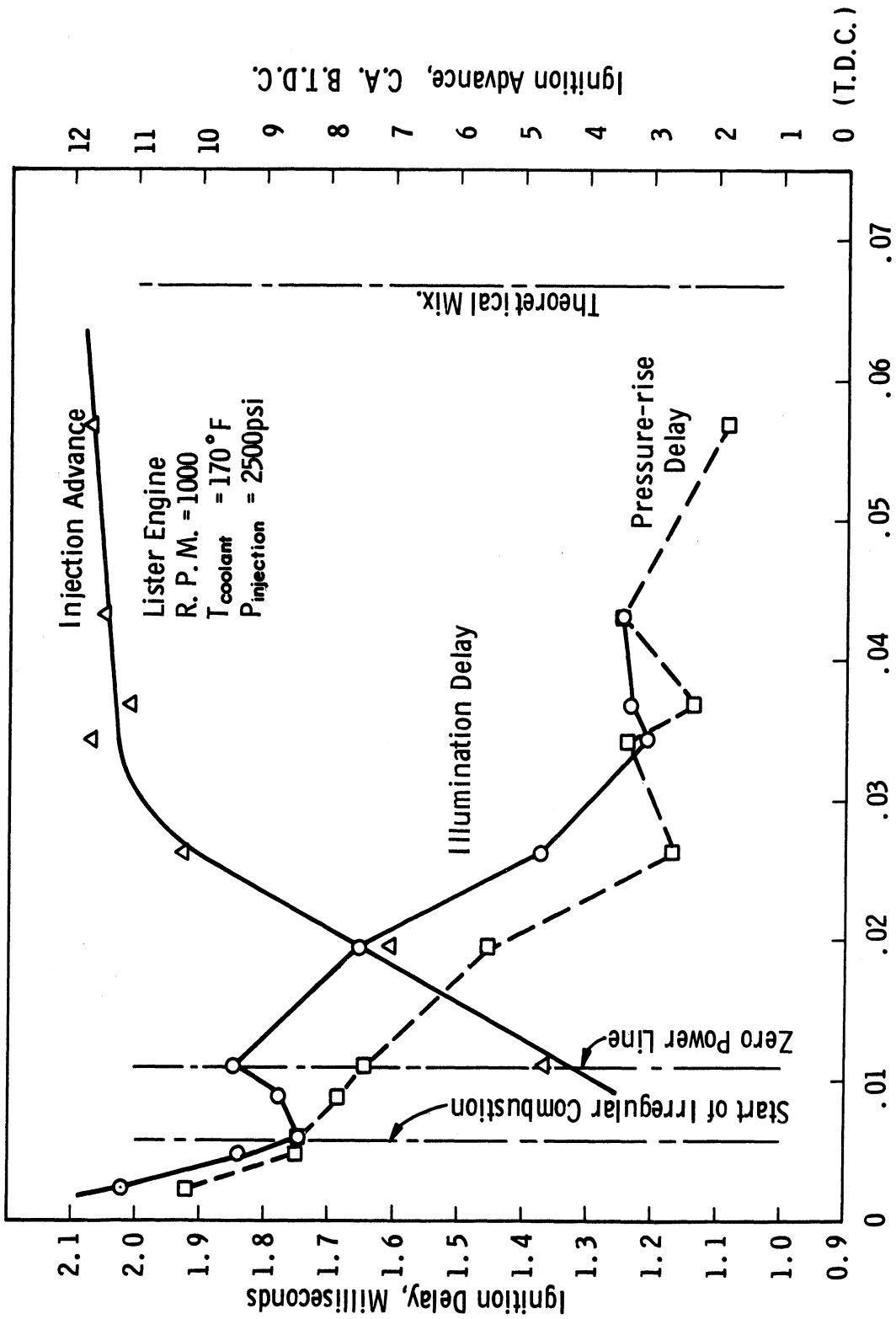


Figure 3. Effect of fuel-air ratio on ignition delay, and injection advance.

The earlier injection at higher fuel-air ratios is believed to be due to the leaking characteristics of the plunger-barrel assembly in the fuel pump. Although the clearance between the plunger and barrel is very small yet the path of the fuel from the high pressure region to the ports changes with the relative position of the plunger-helix with respect to the barrel ports. At high loads, the path of the fuel is long and the leakage is less. Another factor that may anticipate in the fuel injection advance is the throttling effect at the opening and closing of the ports.

The injection advance at high fuel-air ratios can be eliminated by retarding the injection timing. This is not feasible in the Lister engine, but will be possible with the new ATAC engine.

The effect of fuel-air ratio on B.S.F.C. and I.S.F.C. is shown in Figure 4. An increase of fuel-air ratio from 0.11 to 0.0568 caused an increase of 52% in I.S.F.C. The increase in I.S.F.C. with fuel-air ratio, in spite of the earlier injection and shorter delay indicates that ignition delay has no significance to the overall combustion efficiency.

C. EFFECT OF INJECTION PRESSURE ON IGNITION DELAY

In Section B of this experimental work the effect of the fuel concentration on ignition delay was investigated quantitatively. In this part the quality of the fuel-air mixture will be studied as far as its effect on ignition delay.

It is known that many factors influence mixture formation in the diesel engine, including the mean spray velocity at the nozzle, atomization, penetration, evaporation, and mixing with air. Among the factors that substantially affect the mixture formation especially at beginning of the injection process, is the differential pressure across the nozzle orifice. The fuel pressure before the nozzle is primarily a function of the setting of the needle opening pressure. In order to investigate the effect of changing the fuel-air mixture state or quality in the cylinder the opening pressure was changed from 1000 psi to 4000 psi. The effect on ignition lag and S.F.C. are shown in Figures 5 and 6, respectively. Figure 5 indicates that as the injector opening pressure is increased starting from 1000 psi both the illumination and pressure-rise delays are reduced reaching a minimum at a pressure of 2300 and 2500 psi, respectively. At higher injection pressures the ignition lag is again increased.

This is expected, because in a heterogeneous mixture, such as that of the diesel engine, the fuel-vapor concentration depends upon the rate of evaporation of the spray droplets and their orientation in the combustion chamber. A study of the process of injection and spray formation indicates that, for an injector similar to that used in the Lister engine, the spray atomization and penetration depend greatly on the injection pressure. The higher the injection pressure, the more the degree of atomization and the less the penetration. At pressures near 4000 psi, the fuel takes the shape of a finely atomized spray,

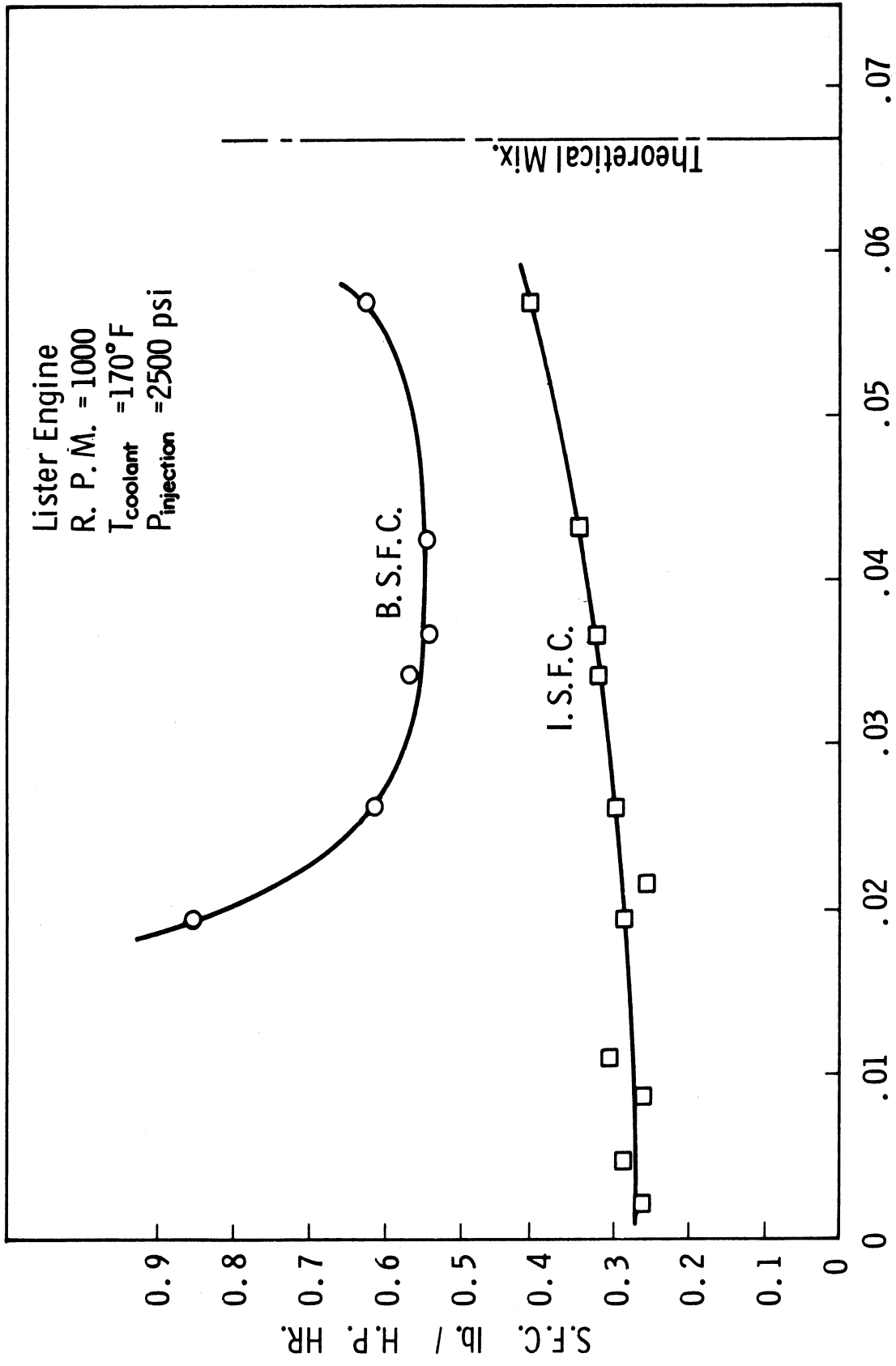


Figure 4. Effect of fuel-air ratio on B.S.F.C. and I.S.F.C.

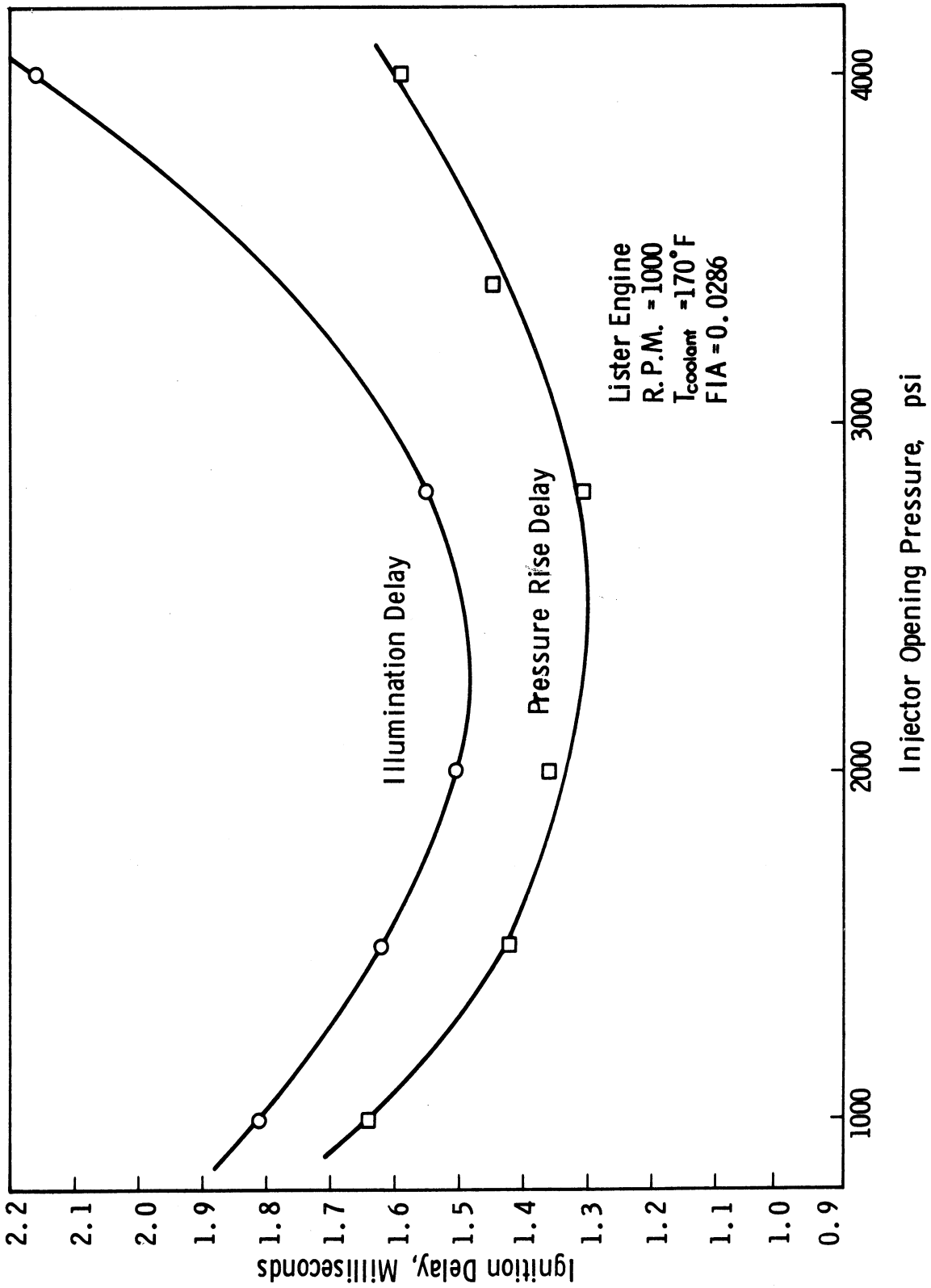


Figure 5. Effect of injector opening pressure on ignition delay.

concentrated near the injection nozzle forming a rich mixture in this area. The far parts of the chamber are left without fuel. This type of fuel distribution caused by changes in injection pressure caused the increase in ignition delay at the higher injection pressures.

The effect of the injection pressure on combustion efficiency is indicated in the I.S.F C. curve, Figure 6. It shows that best efficiency is obtained at injection pressure giving minimum delay.

D. EFFECT OF SURFACE TEMPERATURE ON IGNITION DELAY

Since the air temperature and pressure at the point of injection are functions of the rate of heat loss to the walls as indicated in Section A of this experimental work, it is to be expected that cooling water temperature would affect ignition delay. To investigate this point a series of tests were carried out on the engine at various cooling water temperatures ranging from 70°F up to 200°F. The results are plotted in Figure 7 and indicated that at higher temperatures the ignition delay is reduced. The reduction in pressure rise delay was consistent and amounted to 20% by increasing the cooling temperature from 70 to 200°F.

The cooling water temperature did not only affect the ignition delay, but also it affected the start of injection. Figure 8 shows this effect and an advance of two crank angle degrees was caused by decreasing the water temperature from 200°F to 70°F. This is of special interest in studies of cold starting problems.

E. EFFECT OF TURBULENCE ON IGNITION DELAY

Very little work has been done, in previous investigations to find the effect of turbulence on ignition delay. This is believed to be due to the complicated effect of turbulence on heat exchange between the gas and the walls, injection and vaporization, distribution of the vapor in the chamber. In the Lister engine the turbulence at the end of the compression stroke is caused by forcing the air through the tangential passage between the main chamber and the spherical chamber, as shown in Figure 9.

At the compression ratio used for the present series of runs (13.92:1), the volume of the chamber is equivalent to 6.55% of the total swept volume, and the area ratio of the connecting passage to the piston area is 3.22%. With this configuration, the air in the passage is estimated to obtain velocities as high as 164 fps during the compression stroke, at an engine speed of 1000 rpm (Reference 1). The air speed in the passage at different crank angles is shown in Figure 10.

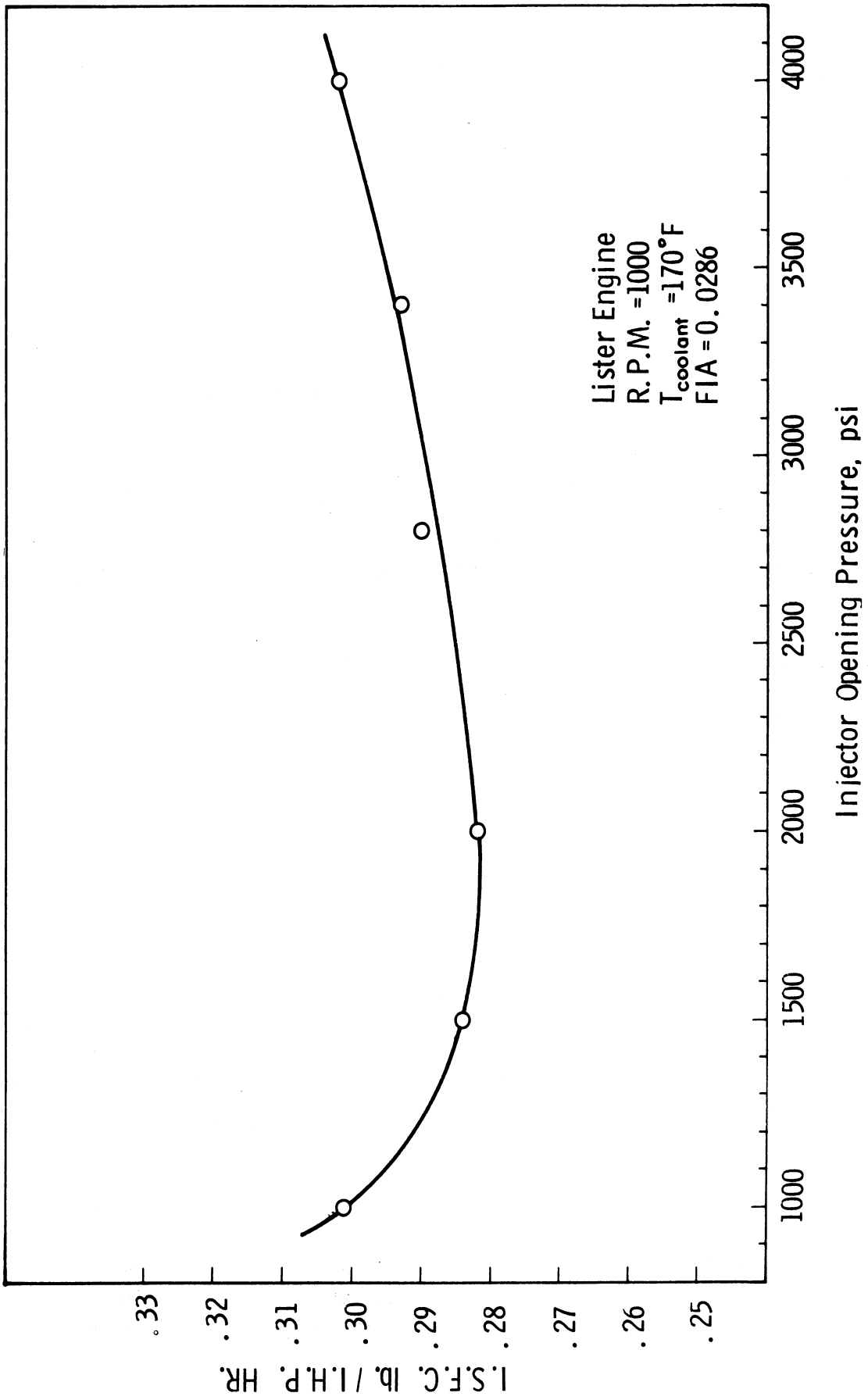
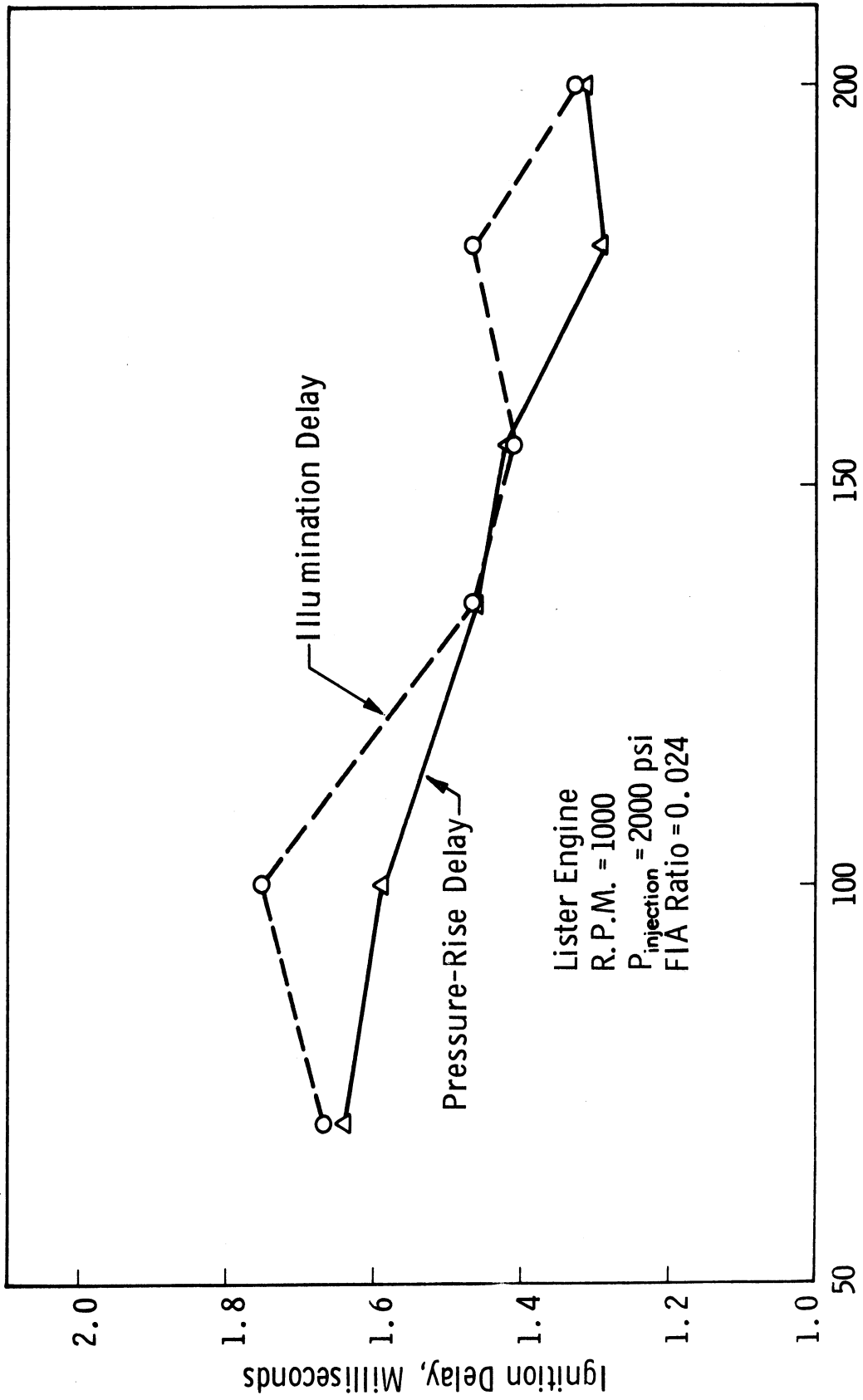


Figure 6. Effect of injector opening pressure on I.S.F.C.



Cooling Water Temperature °F at Outlet

Figure 7. Effect of cooling water temperature on ignition delay.

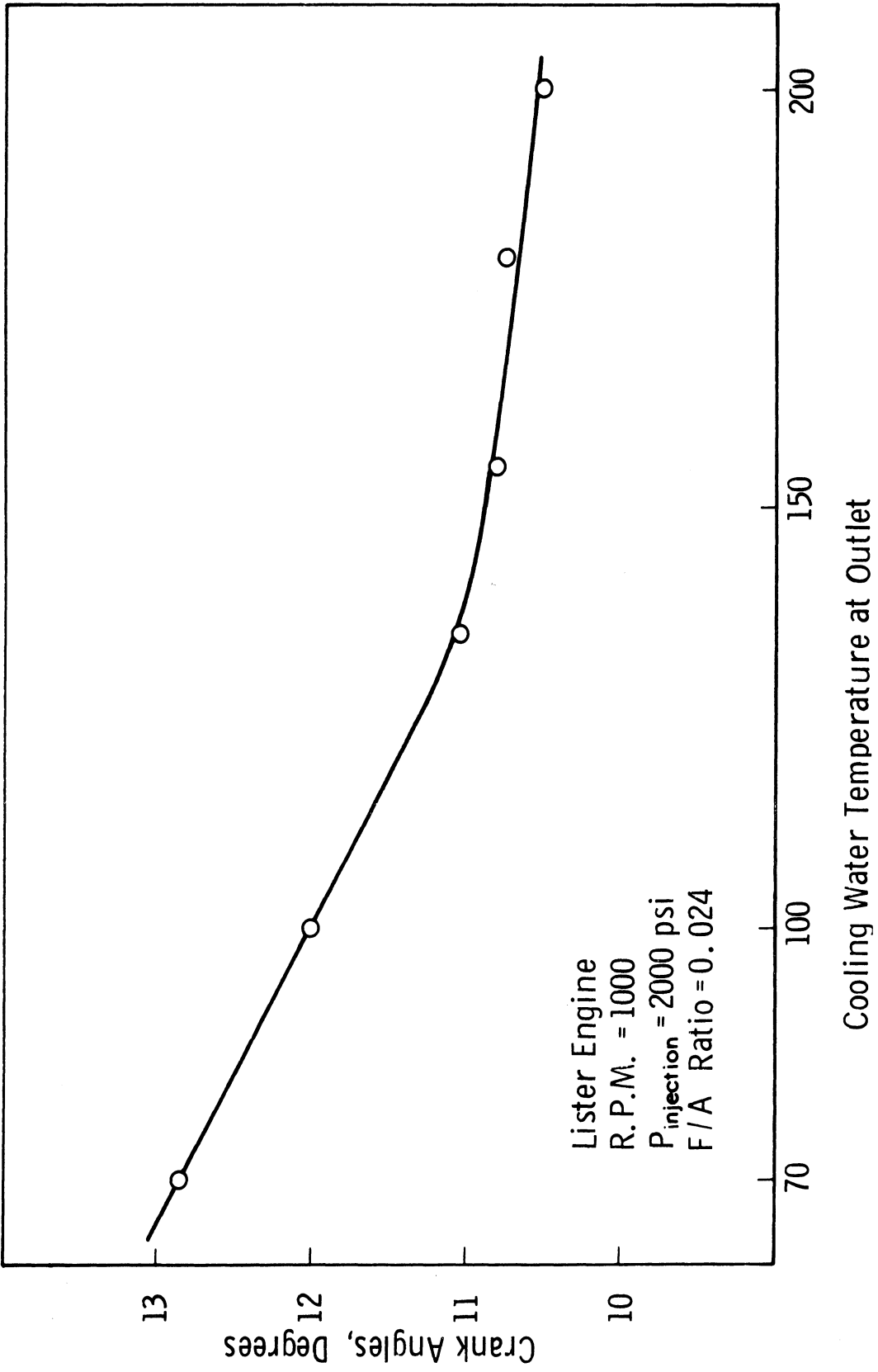


Figure 8. Effect of cooling water temperature on injection start.

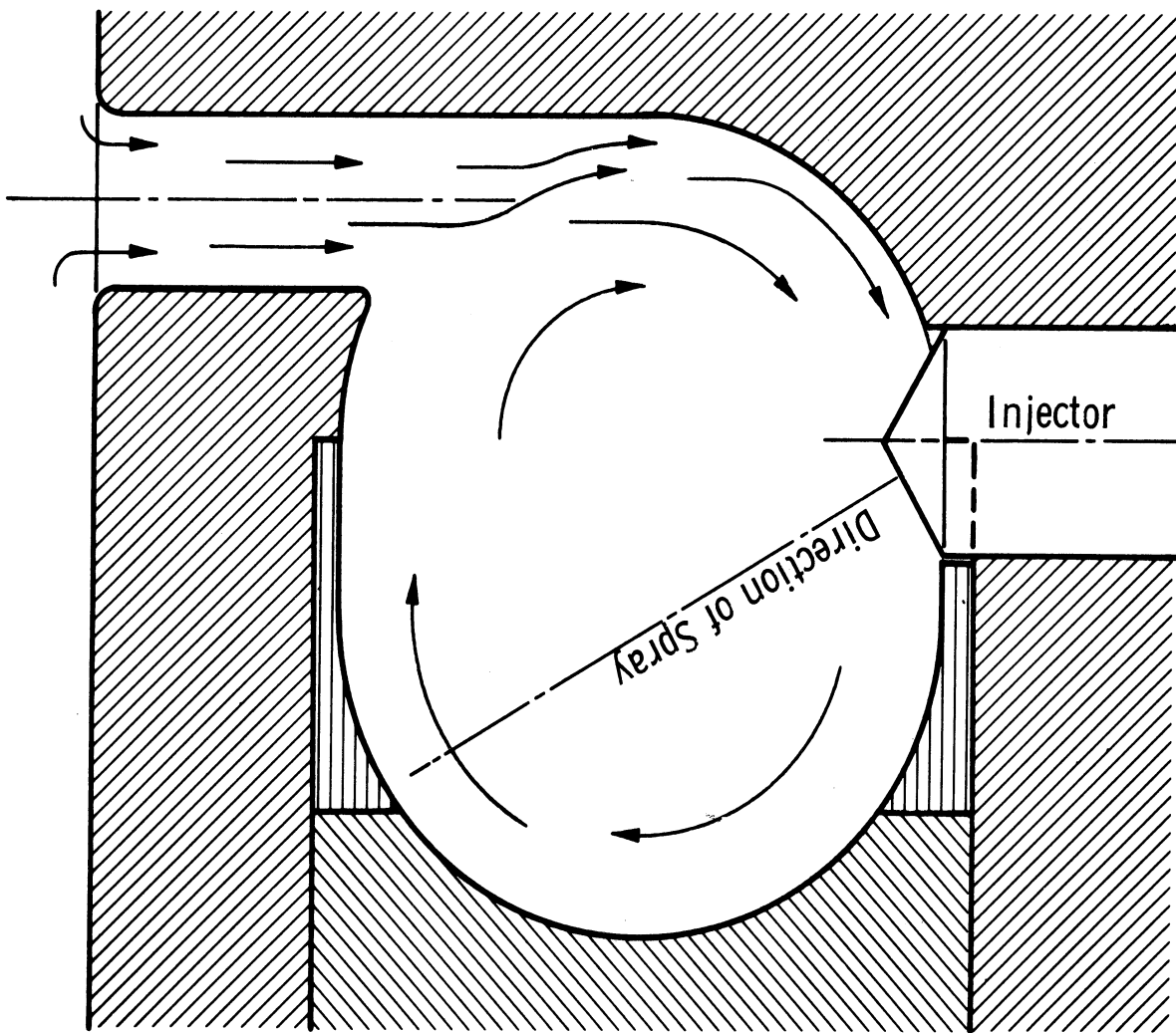


Figure 9. Turbulence in modified combustion chamber of Lister engine.

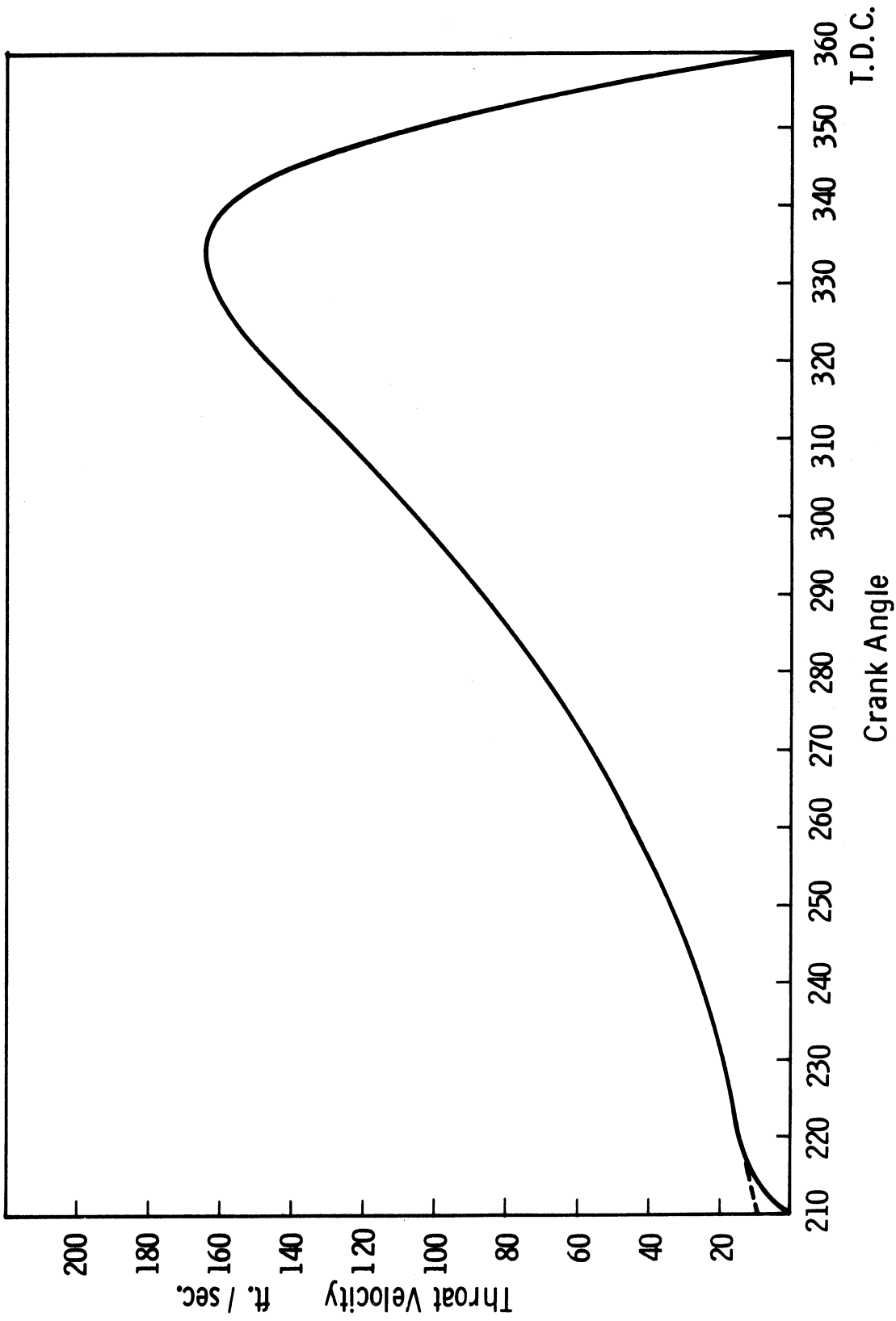


Figure 10. Air speed in the tangential passage to the swirl chamber of Lister engine at 1000 rpm.

The effect of increased speed on decreasing the illumination and pressure-rise delays is shown in Figures 11 and 12.

It is noticed that both ignition delays increase in terms of crank degrees and decrease in terms of milliseconds. An increase of engine speed from 500 rpm to 1200 rpm caused a drop of 28% in illumination delay and 40% in pressure rise delay. The effect of increased turbulence on the specific fuel consumption is shown in Figure 13.

It is to be noted that the increase in turbulence, caused by increasing engine speed, is not the only factor that is responsible for the decrease in delay period. Other factors are the increase in air pressure and temperature at higher speeds. However, this is partially counteracted by the effect of injecting the fuel earlier in the compression stroke, i.e., at temperatures and pressures lower than those that might occur nearer to T.D.C. The injection advance at the different speeds is measured from the traces and plotted in Figure 14.

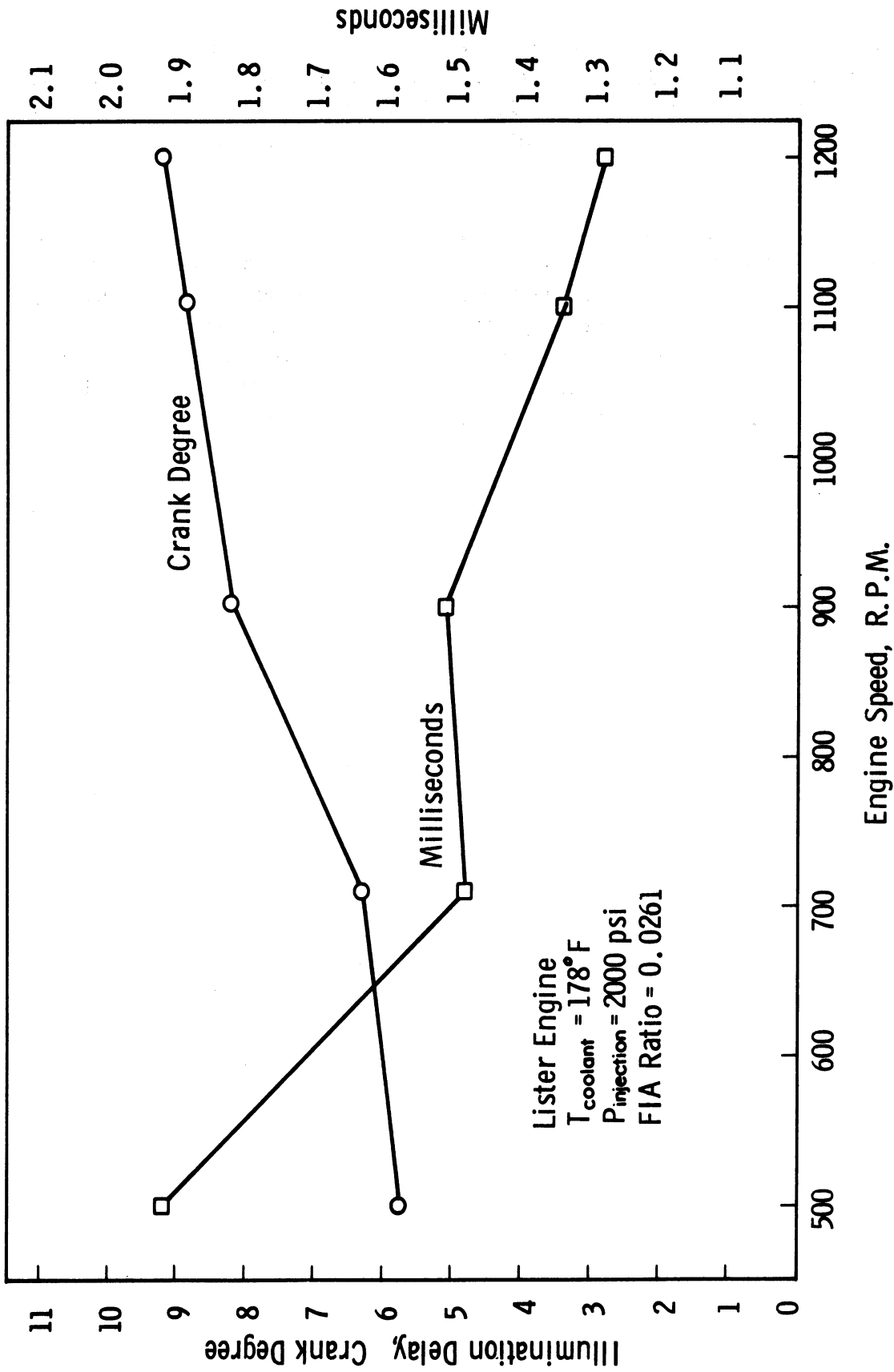


Figure 11. Effect of engine speed on illumination delay.

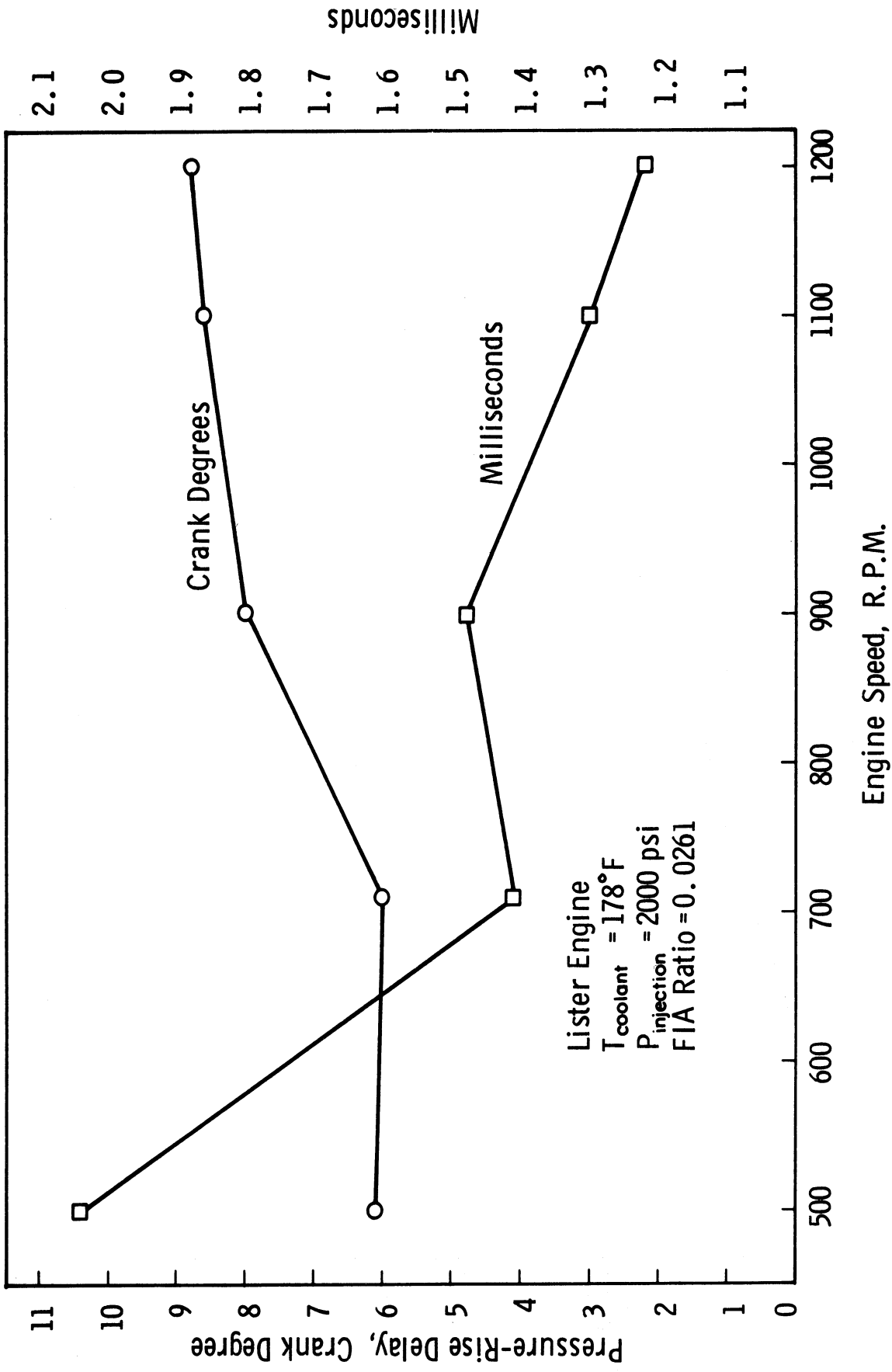


Figure 12. Effect of engine speed on pressure-rise delay.

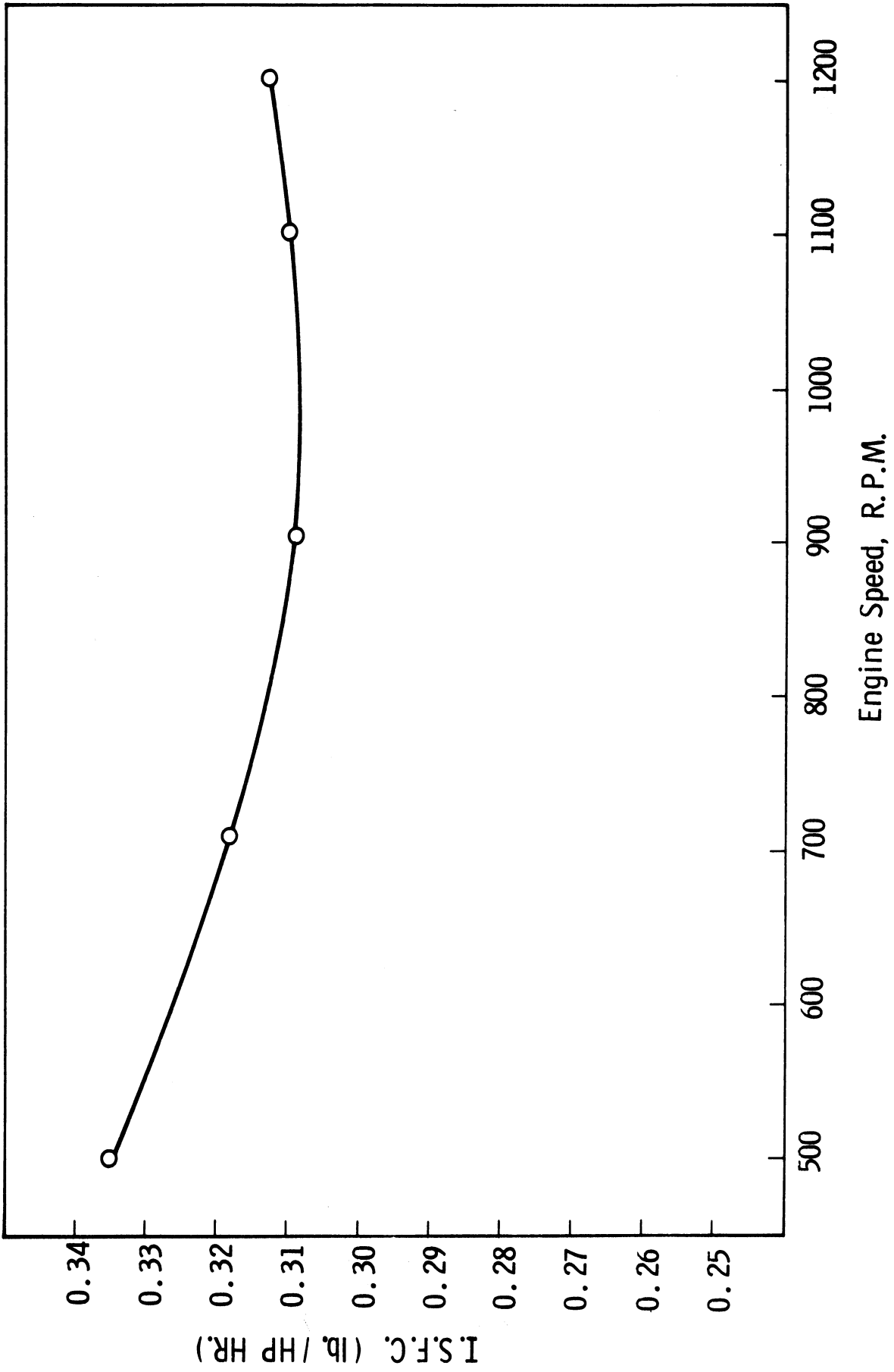


Figure 13. Effect of engine speed on I.S.F.C.

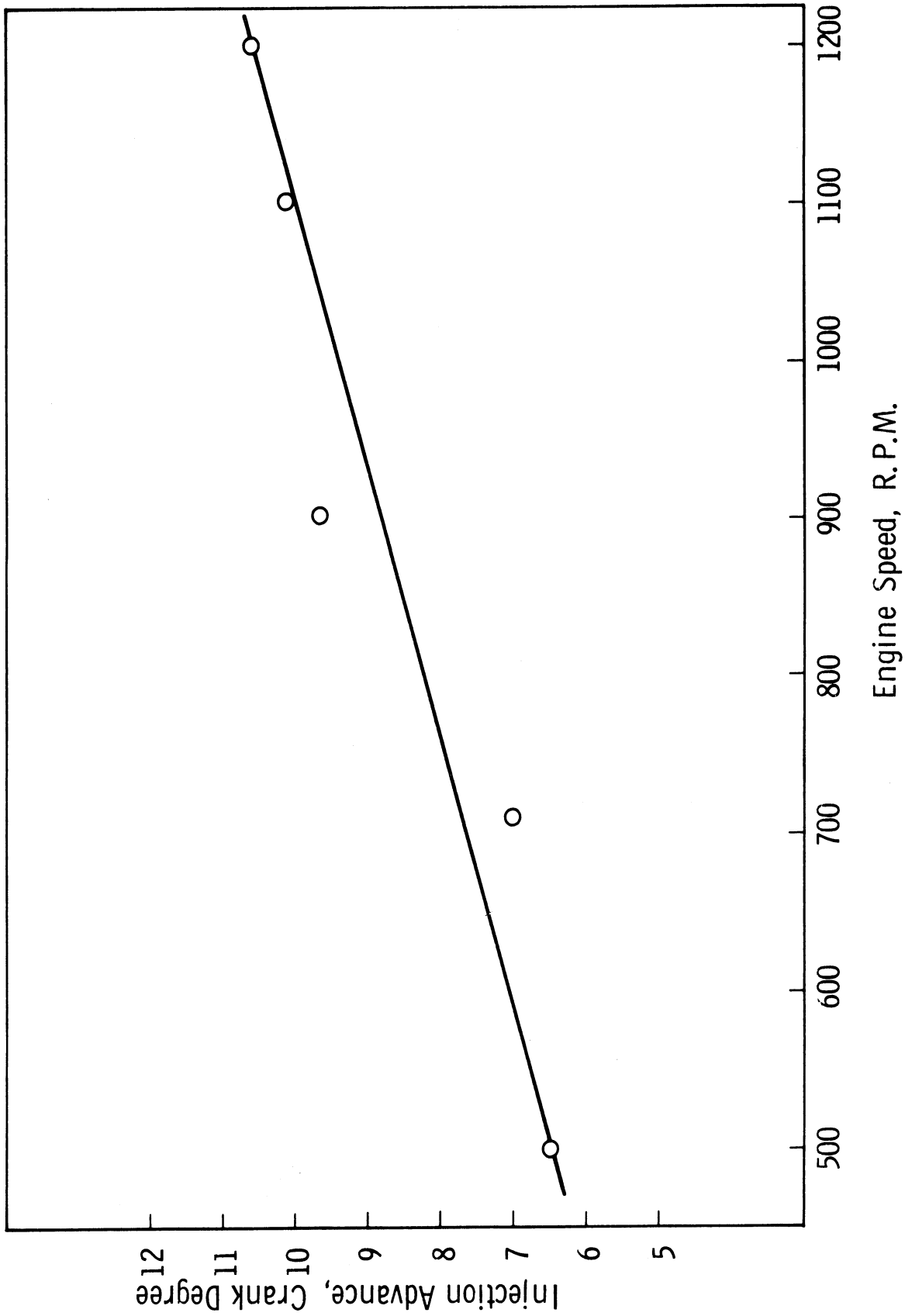


Figure 14. Effect of engine speed on injection advance.

COMPUTATIONS

These computations are based on the experimental measurements taken while testing the engine under the conditions given in Appendix I.

A. GAS TEMPERATURE

The average gas temperature at any point in the cycle was calculated from the measured air flow, fuel flow, and the cylinder pressure, by using the equation of state. The gas temperature is shown in Figure 15, together with the gas pressure.

B. RATE OF HEAT RELEASE

The rate of heat release was derived from the first law of thermodynamics, Appendix III, and is given by:

$$\frac{dQ}{d\theta} = \left(\frac{c_v}{R} + \frac{1}{J}\right) P \frac{dV}{d\theta} + \left(\frac{c_v}{R}\right) V \cdot \frac{dP}{d\theta} \quad (9)$$

The values computed for the rate of heat release and accumulated heat release are plotted in Figure 16. This figure indicates that there is a negative heat release when injection first starts at 356 crank degrees, or 4° before T.D.C. This is probably due to heat losses to cylinder walls and in heating up and evaporating the fuel. The rate of heat release reaches zero at 2.5° before T.D.C. indicating that the amount of energy produced from the reaction is just enough to balance the heat losses from the gas to the walls. The maximum value of heat release is 0.0395 BTu/crank degree at a crank angle of 373, after which it drops continuously till the start of after-injection. The increase in the heat release rate between 390 and 420 seems to be due to the energy released from the combustion of the after-injected fuel.

This diagram shows also that the heat release continues till near the end of the expansion stroke. This is believed to be due to the very late addition of fuel in the after-injection which continued to an angle of 396. To check the phenomena of heat release near the end of the expansion stroke the P-V relationship was plotted on a log-log sheet, from which the index of each process can be obtained, and the condition of heat transfer to or from the gas is indicated.

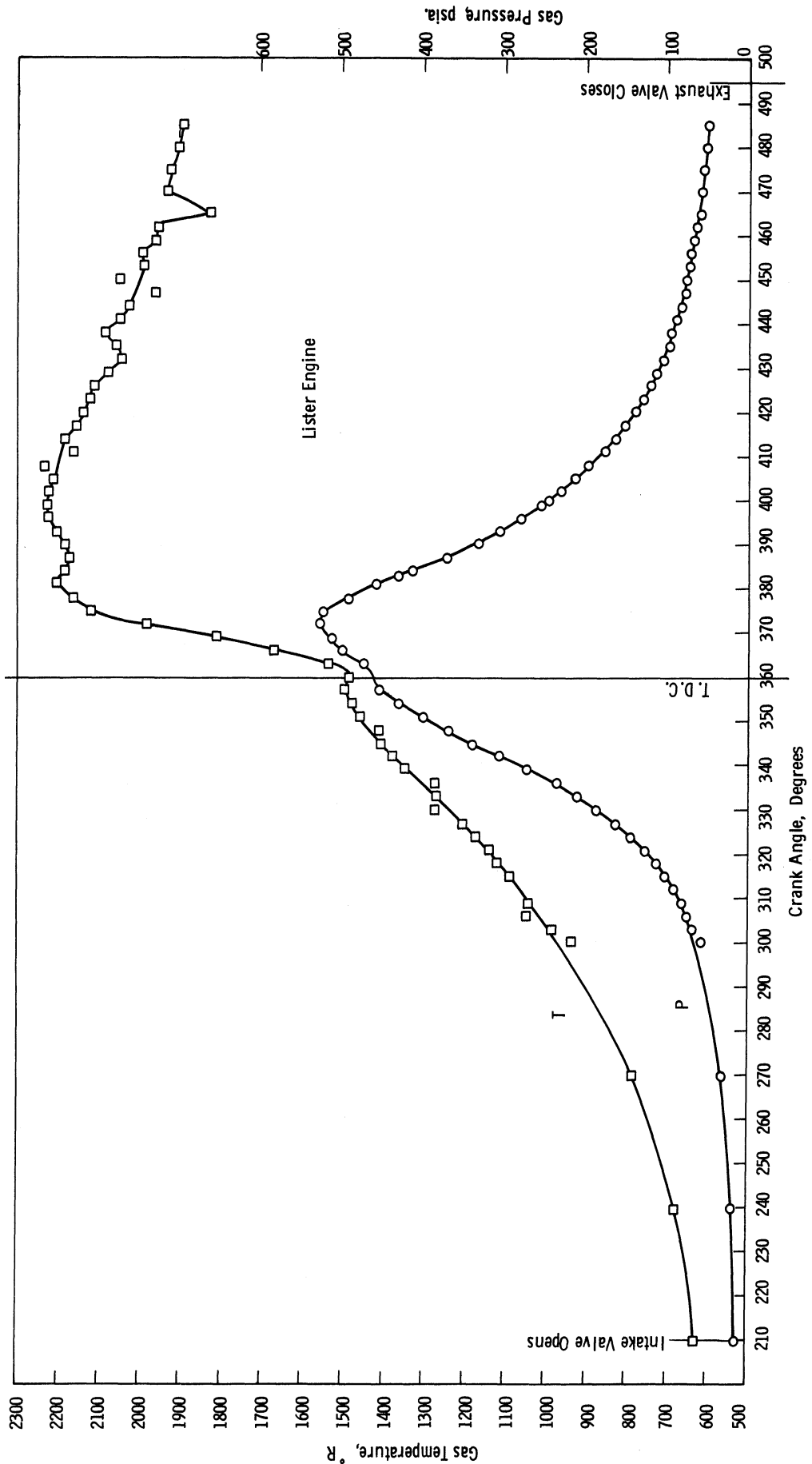


Figure 15. Gas pressure and temperature during the cycle.

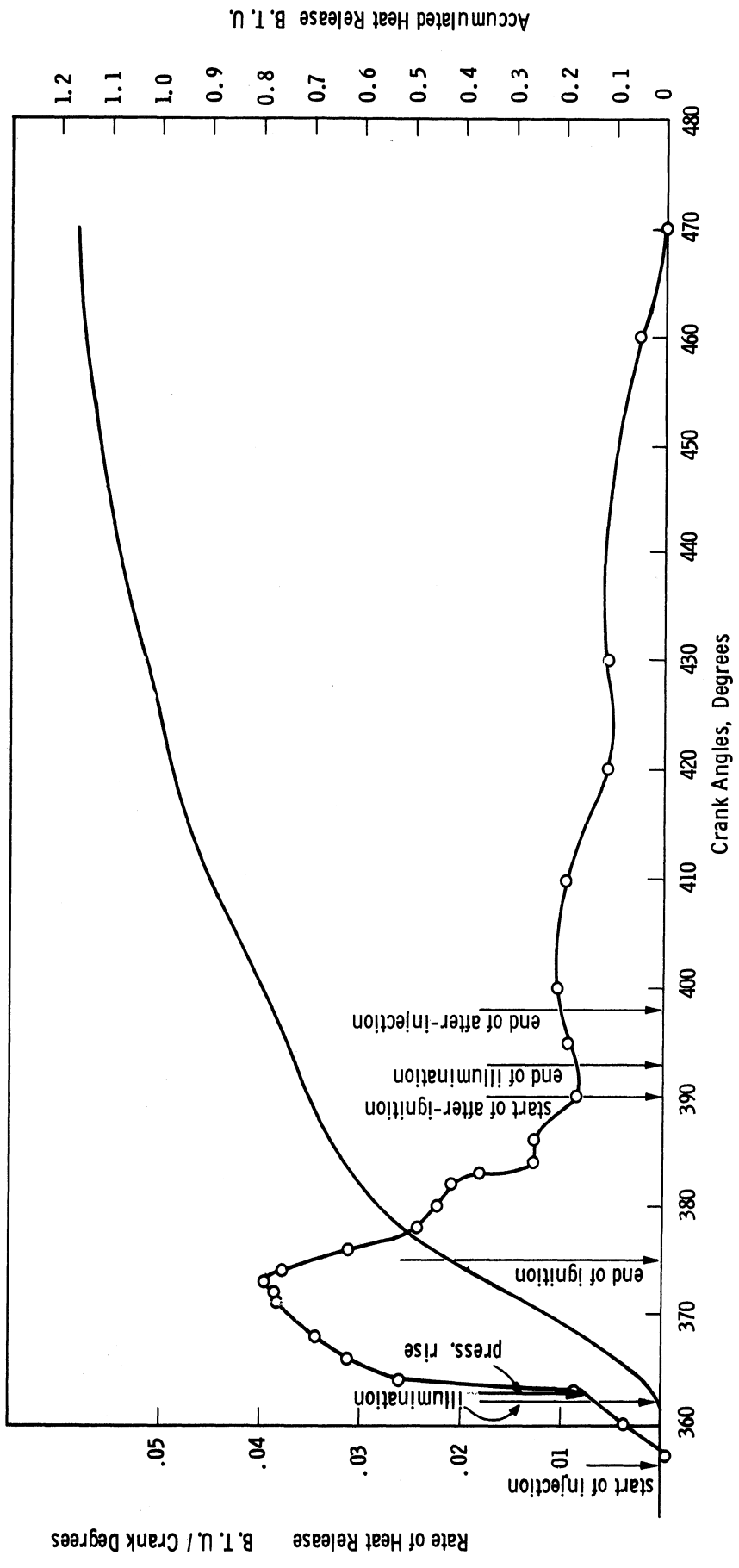


Figure 16. Rate of heat release and accumulated heat release diagrams.

C. INDEX OF COMPRESSION AND EXPANSION

In order to calculate the index of compression and expansion the gas pressure and volume are plotted on a log-log sheet as shown in Figure 17. For the compression stroke the index of compression (the value of n) changed from 1.392 at the early part of the stroke to 1.11 at the end of compression. For the early part of the expansion stroke the index started with a negative value of -1.026, increased to zero shortly after T.D.C., reached 0.99 during the early part of the expansion, and increased to 1.15 at the end of the expansion stroke.

The factors that affect the index of compression and expansion are:

1. the rate of heat release due to combustion
2. the rate of heat exchange between the gas and walls
3. the physical properties of the gas as regards composition and specific heats
4. the blowby rate. In general the blowby rate is small if the cylinder and piston are in good conditions.

At the beginning of compression work is done on the gas, which is still at a temperature lower than wall temperature. The combined effect of compression work and heat gain from the walls result in a value of 1.392 for n . This value is the highest in the whole cycle. The conditions are not the same near the end of compression. Heat is lost to the walls, the specific heats are higher due to increase in temperature and the gas blowby rate is also high. All these factors cause a drop in the value of n to 1.11.

At the beginning of expansion stroke the rate of heat release due to combustion is the dominating factor and $n = -1.026$. The pressure reaches its maximum shortly after T.D.C.

As the piston goes on the expansion stroke, work is done by the gases, but heat is still being released causing index to be 0.99 which is very near to isothermal expansion in which case the net heat added to the gas is equal to work done by the gases. The value of n continues to increase, as the piston proceeds near end of expansion, where it reaches 1.15.

For a polytropic process the heat added to the gases can be given by:

$$dQ = mC_n (T_2 - T_1) \quad (10)$$

where

$$c_n = -c_v \frac{K - n}{n - 1} \quad (11)$$

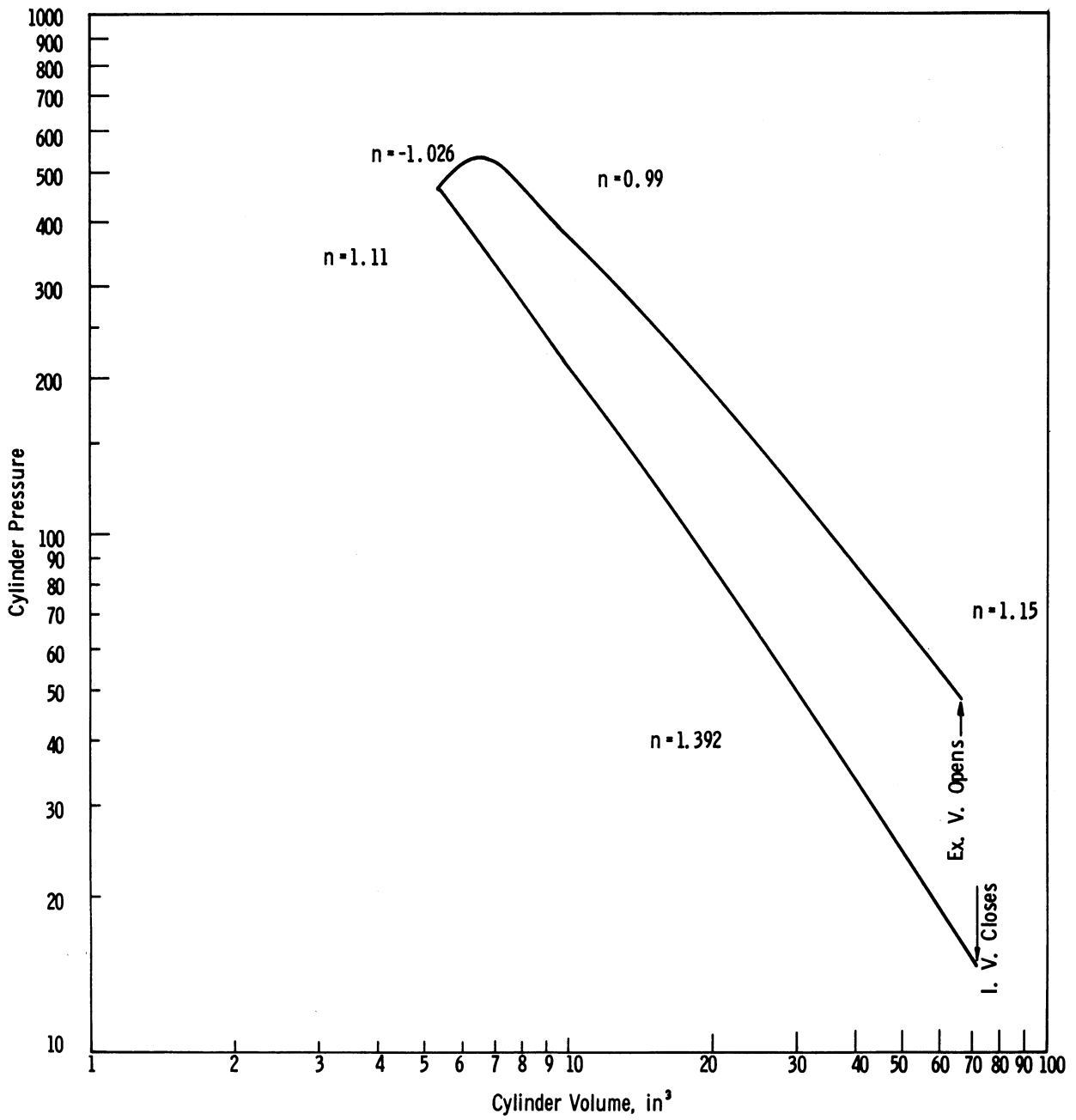


Figure 17. P-V relationship on a Log-Log sheet.

T_2 and T_1 are the gas temperatures at the end and beginning of the process consecutively.

Near the end of the expansion stroke $K = 1.315$, and $n = 1.15$ (obtained from the log-log sheet). Therefore according to equation (10) some heat should be released. This conclusion supports the results of the heat release computations.

D. RATE OF FUEL INJECTION

The rate of fuel injection into the cylinder was computed from the pressure difference across the nozzle, the area of flow, and a coefficient of discharge c_d .

$$m_f = c_d A_f \sqrt{2g \zeta_f (P_f - P_g)} \quad (12)$$

The value for c_d was computed from the measured fuel consumption and the accumulated fuel injection, as calculated from Equation (12) with $c_d = 1$. The value obtained for c_d is 0.891. It is to be noted that the coefficient of discharge depends on the general form of the orifice, the ratio of its length and diameter and the injection pressure. In our case the ratio of length to orifice diameter is equal to 6.4. By referring to values for c_d , obtained by previous investigators for similar orifices, under the same injection pressures, it was found to be 0.88 (4).

Figure 18a is a cross section in the nozzle-needle assembly. Figure 18b indicates that the area of flow between the needle and seat is smaller than the orifice area for lifts less than 0.0008 in. For higher lifts the area of flow is limited by the orifice area which equals 0.0000865 in².

The rate of fuel injection and the accumulated injected fuel at different crank angles are calculated and plotted in Figure 19. From this figure it is noticed that after injection started at an angle of 389°, or 14 crank angle degrees after the end of the first injection.

E. COMBUSTION COMPUTATIONS

The experimental results for this sample run are as follows:

Start of injection	=	4.2 B.T.D.C.
Illumination (solar cell)	=	2 A.T.D.C.
Pressure rise	=	2.5 A.T.D.C.
Illumination delay	=	6.2°C.A.
	=	<u>1.03 millisec.</u>
Pressure rise delay	=	<u>1.117 millisec.</u>

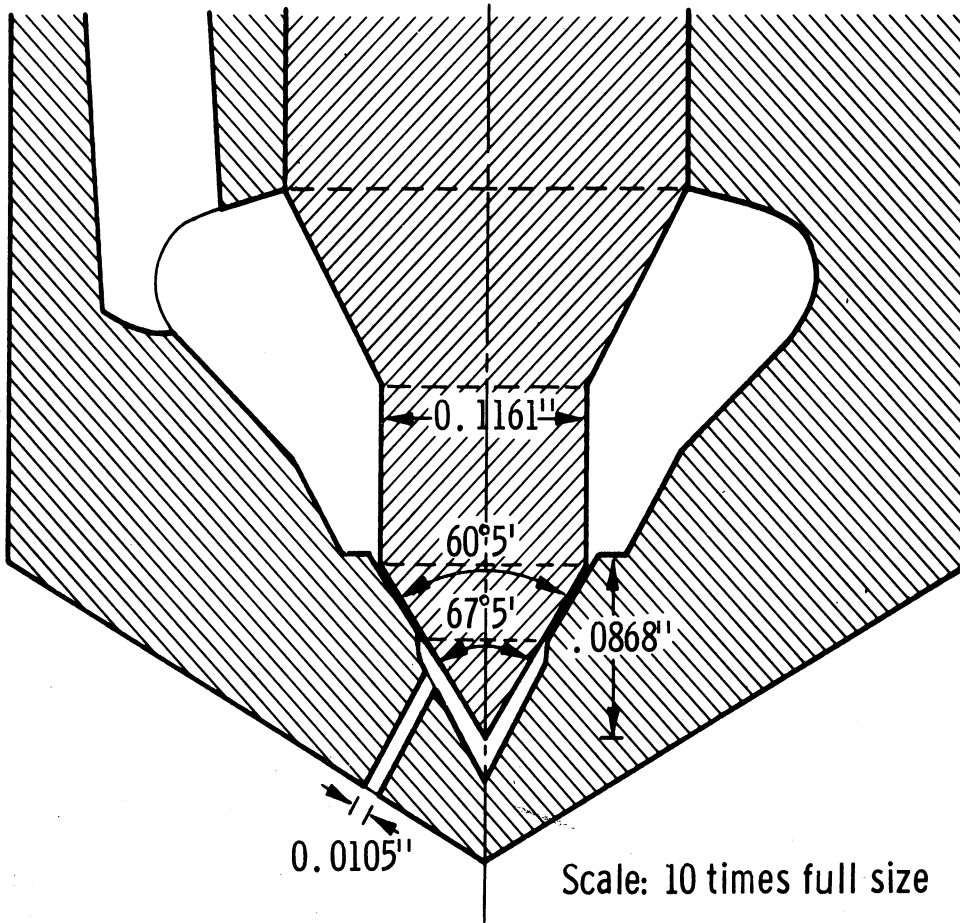


Figure 18A. Nozzle needle assembly.

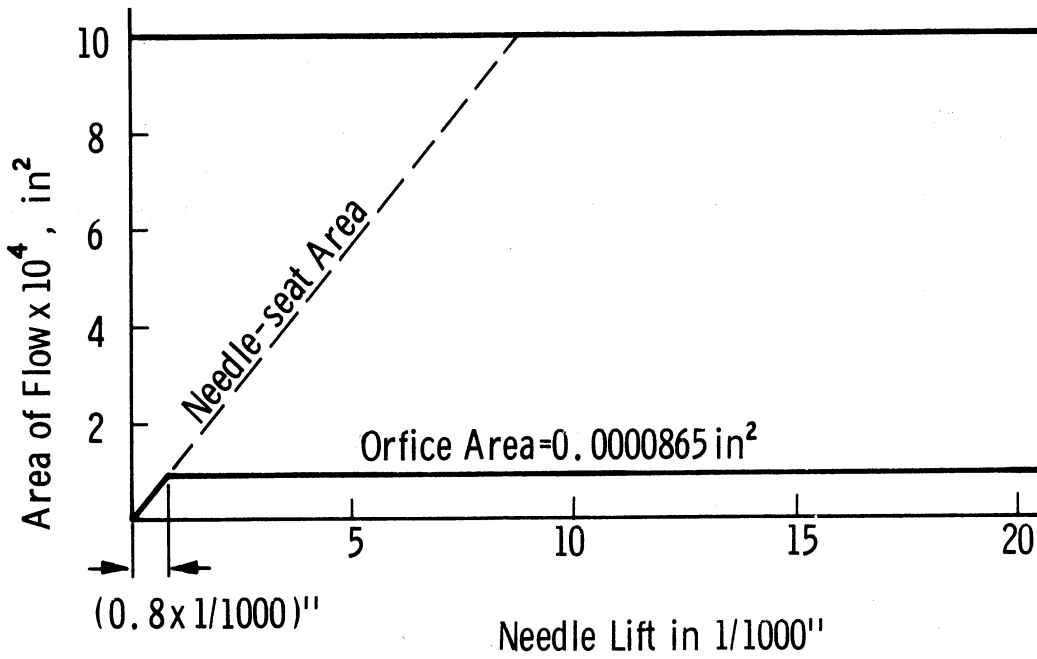


Figure 18B. Area for fuel flow vs. needle lift.

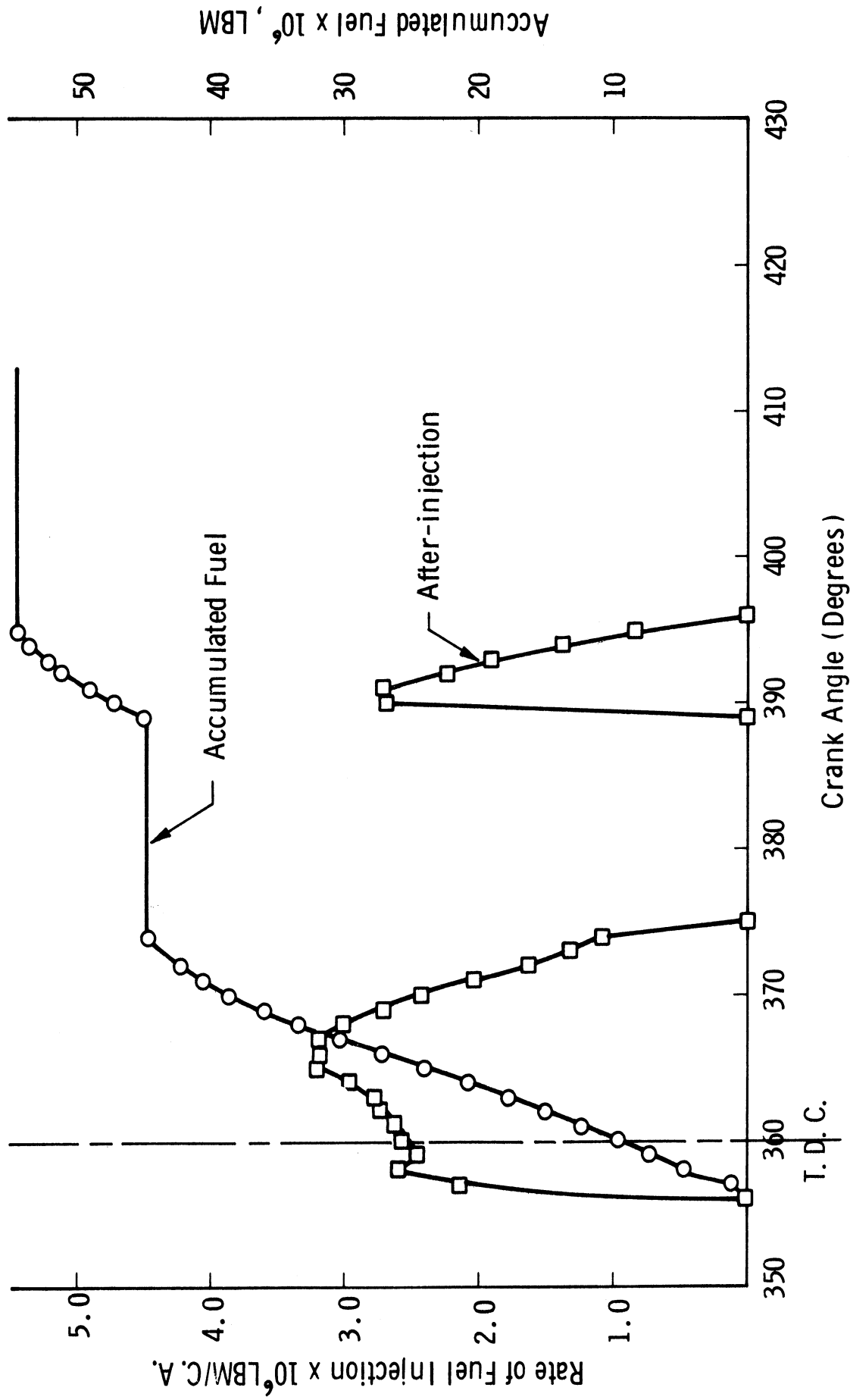


Figure 19. Rate of fuel injection and accumulated fuel diagrams.

By applying the different formulae for the delay period the following results are obtained:

Wolfer's Formula

$$\text{Pressure rise delay} = \underline{2.98} \text{ milliseec.}$$

Bauer's and West Formula

$$\begin{aligned} & \text{(from Figure 1) at } T \log P & = 2180, \\ \text{Pressure rise delay} & & = \underline{1.5} \text{ milliseec.} \end{aligned}$$

Tsao, Myer's, and Uyehara Formula

$$\text{Temperature rise delay} = \underline{2.11} \text{ milliseec.}$$

CONCLUSIONS

The ignition delay period has most commonly been taken to be the elapsed time from the beginning of injection to the point where measurable pressure rise due to combustion occurs. Some research workers have also measured the time until illumination due to burning began, and others have noted the start of temperature rise due to burning. However, a review of this work shows that little discussion and comparison has been made between the different delay periods. Measurements have been made for this project of the period from the beginning of injection until measurable pressure rise due to combustion occurs, and until illumination due to burning occurs. These measured time intervals are usually different. Therefore, for a thorough study of the diesel ignition delay and combustion process, it seems desirable to observe and report each of them. Consequently, the ignition delay has been identified as 'pressure rise,' 'temperature rise,' or 'illumination delay.' Because the 'temperature rise' is very difficult to measure, our future studies will only include 'pressure rise' and 'illumination delay.'

The formulae available for the ignition delay are based on test data relating to a specific set of engine conditions. However, it has been established that a large group of variables other than air pressure and temperature have a significant effect on the ignition delay. These include the fuel concentration in the air, the conditions of the spray as regards its atomization and orientation in the chamber, the air turbulence, and the cylinder wall temperature.

The results of the experimental part of this work indicated that the increase in fuel-air from 0.011 to 0.043 caused a drop of 32% in the illumination delay. An increase in fuel-air ratio from 0.011 to 0.0568 caused a drop of 34% in the pressure rise delay. The results of the experiments carried out to investigate the effect of the degree of atomization and penetration indicated that both the pressure rise and illumination delays reach a minimum value at a nozzle opening pressure of about 2400 psi. The results of experiments at different cooling water temperatures indicated that a reduction in water temperature from 200°F to 70°F caused an increase of 20% in pressure rise delay. The effect of turbulence was studied by varying the engine speed. An increase in engine speed from 500 rpm to 1200 rpm caused a drop of 28% in illumination delay and 40% in pressure rise delay.

In future runs for the determination of the effect of pressure, temperature on ignition delay the conditions of the test as regards fuel-air-ratio, injection pressure, coolant temperature and engine speed will be kept constant and recorded.

RECOMMENDATIONS

Since the Lister engine and associated equipment which had been used in this investigation have proved to be very useful for this project, it is recommended that we continue to operate this set-up while installing and operating the army A.T.A.C. engine. This will help us to obtain information on a divided combustion chamber system. Comparison of the test results of this engine with the open chamber A.T.A.C. engine will be of great value in studying the combustion phenomena in diesel engines.

Another important advantage of the Lister engine is the large access hole into the combustion chamber, having a diameter equal to that of the swirl chamber. This has permitted us to have three extra access holes to the combustion chamber, and to use a large quartz window to photograph the combustion phenomena.

The Lister set-up is instrumented to obtain information on the effect of pressure, temperature, and density on ignition lag of different fuels. It also allows measurement of the ignition lag at four compression ratios in the range 14:1 to 22:1. In the present tests a C.R. of 14:1 has been used to avoid interruption of work due to engine failure that might occur at the high compression ratios. It is believed that the tests of different fuels at higher C.R. will be of great value for this research, especially to determine if density is an independent variable affecting ignition delay.

APPENDIX I

INSTRUMENTATION IMPROVEMENT

During the course of running the tests to investigate the effect of the different parameters on ignition delay, it was noticed that some improvements on instrumentation can be made. However, it was decided to continue these tests with the same instruments as mentioned in a previous report, Ref. 2, in order to make a comparative study on the effect of the different parameters on the ignition delay. These improvements are still on the way and have been made as an attempt to determine more precisely pressure rise and illumination delays, and to eliminate the error caused by cycle to cycle variations. A definite conclusion about the superiority of some of them over the instruments now in use is not reached yet as the work is still on the way.

A. PRESSURE-RISE DELAY

The point at which pressure rise due to combustion could be found from a pressure differential trace displayed on the oscilloscope screen. The differential circuit used is shown in Figure 20, together with the pressure circuit. The differential trace obtained is shown in Figure 21, together with the pressure trace. It was noticed that there is a phase shift between the two traces.

To study the magnitude of the phase shift between the two traces a series of runs were carried out with the engine motored. The lag of the zero differential pressure behind the maximum pressure at different crank angles was measured and plotted in Figure 22. From this figure the lag is 0.438 millisecc. at 700 rpm and 0.405 millisecc at 120 rpm. It was also noticed that the lag depends to a great deal on the capacitance of the circuit.

Another difficulty encountered with this method was the determination of the point at which the slope change occurs due to combustion.

Due to the above difficulty and phase lag dependence of the system capacity the results of this method seemed not as accurate as that using the pressure trace. The results included in this report are for the pressure rise delay as measured from the pressure trace only.

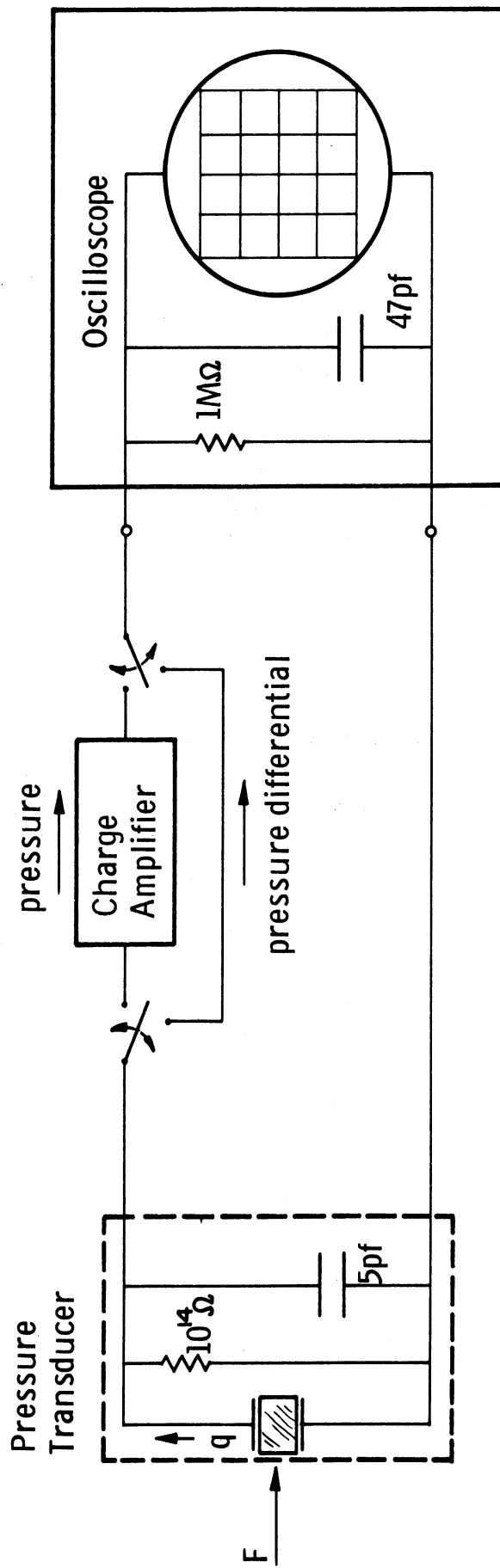


Figure 20. Pressure and pressure differentiating circuit.

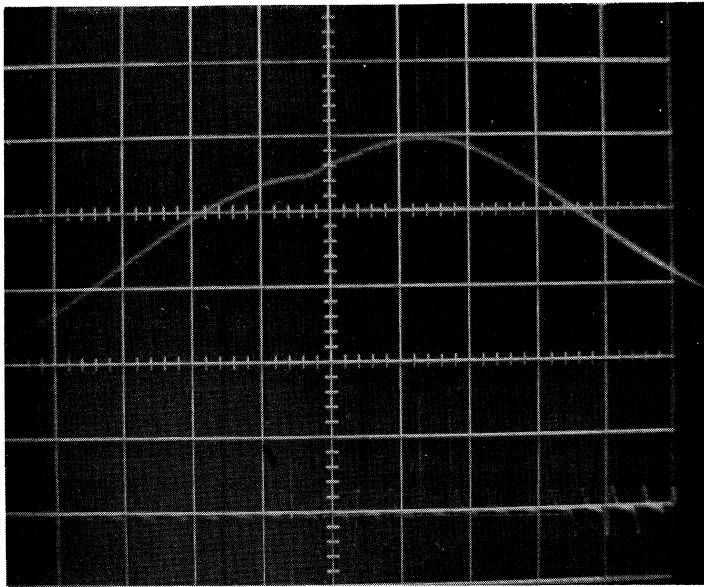


Figure 21A. Pressure trace.

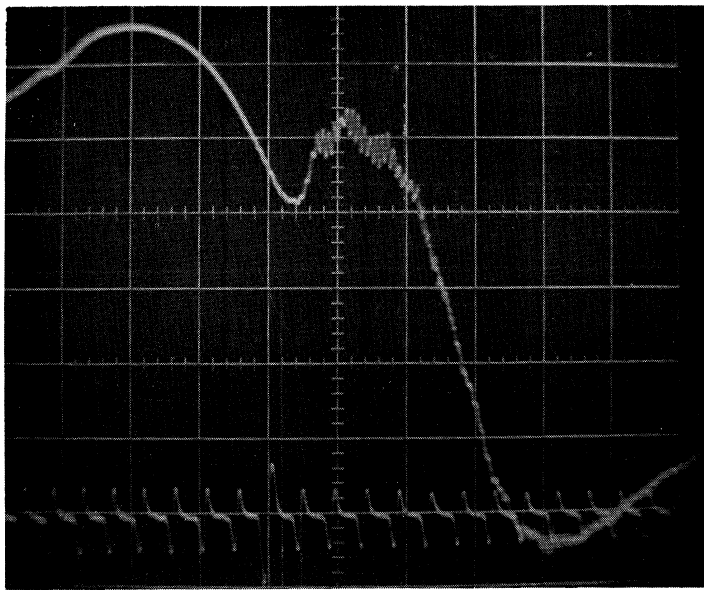


Figure 21B. Pressure differential trace.

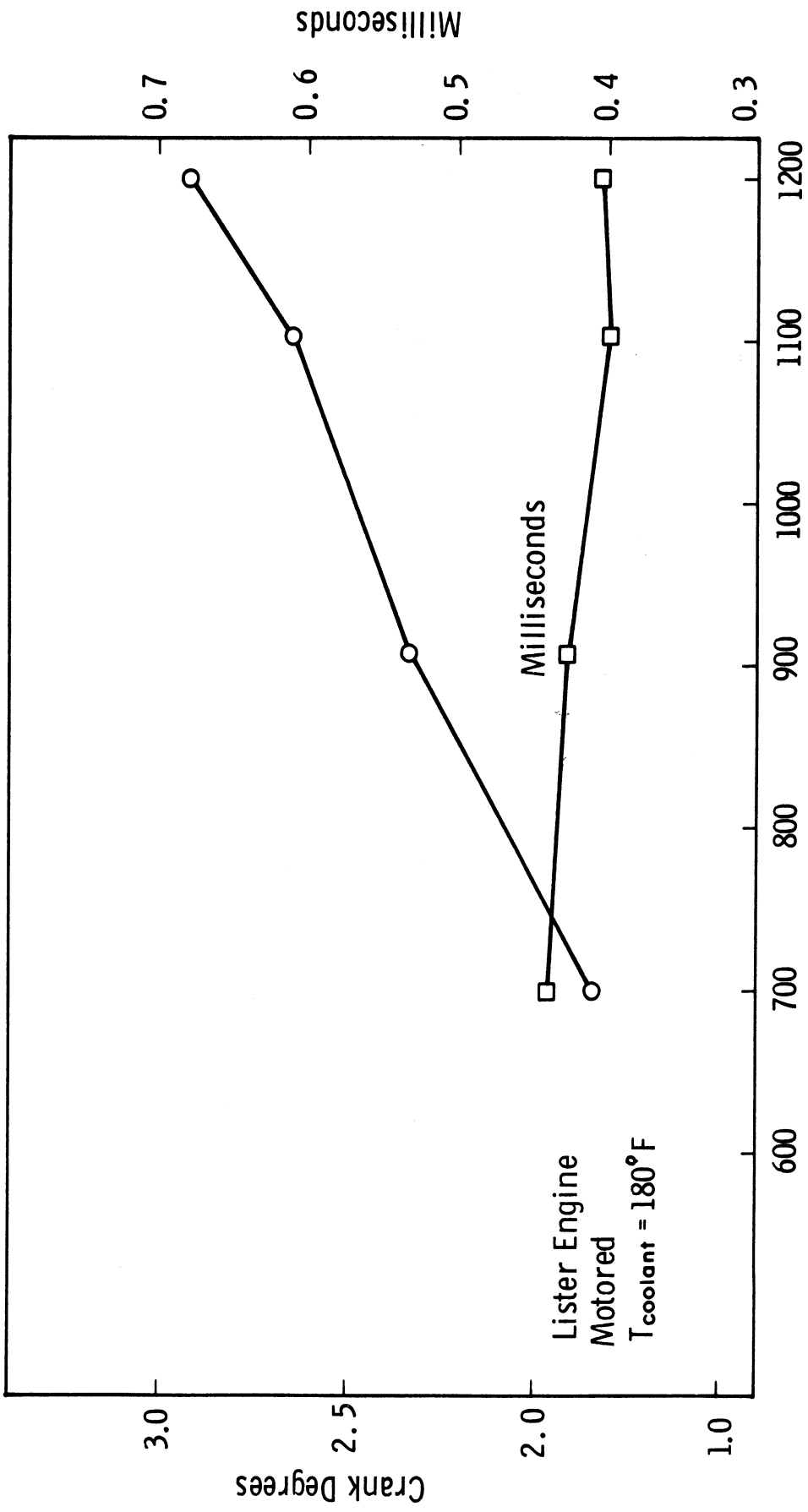


Figure 22. Lag between the pressure and the pressure differentiating circuits.

B. ILLUMINATION DELAY

A study on the possibility of using an instrument more sensitive than the solar cell is now under way. This study was initiated to study in greater detail the reasons for the difference between the measured illumination delay period and the pressure rise period. In some runs we noticed that illumination delay is shorter than the pressure rise delay, while in other runs the opposite was observed.

The instrument we are trying to use is a photomultiplier, which is now being fitted on the combustion chamber of the Lister engine. The results obtained from this instrument will be included in the next report.

Visicorder

Most of the records of combustion phenomena for this project were made with a dual beam oscilloscope and a polaroid camera. In order to eliminate the error caused by cycle-to-cycle variation with these instruments a Honeywell direct recording visicorder, with 12 channels was also used. The signals for gas pressure, crank angles, fuel pressure, needle lift, and solar cell are fed simultaneously to the galvo-amplifiers of the visicorder. The traces obtained are shown in Figure 23. The speed of recording was set at maximum value, 80 in./sec, and the engine speed was as low as 500 rpm. However, such a recording speed was not high enough to obtain traces large enough to give the degree of accuracy required. Consideration is now being given to the purchase of a visicorder with a recording speed of 160 in./sec.

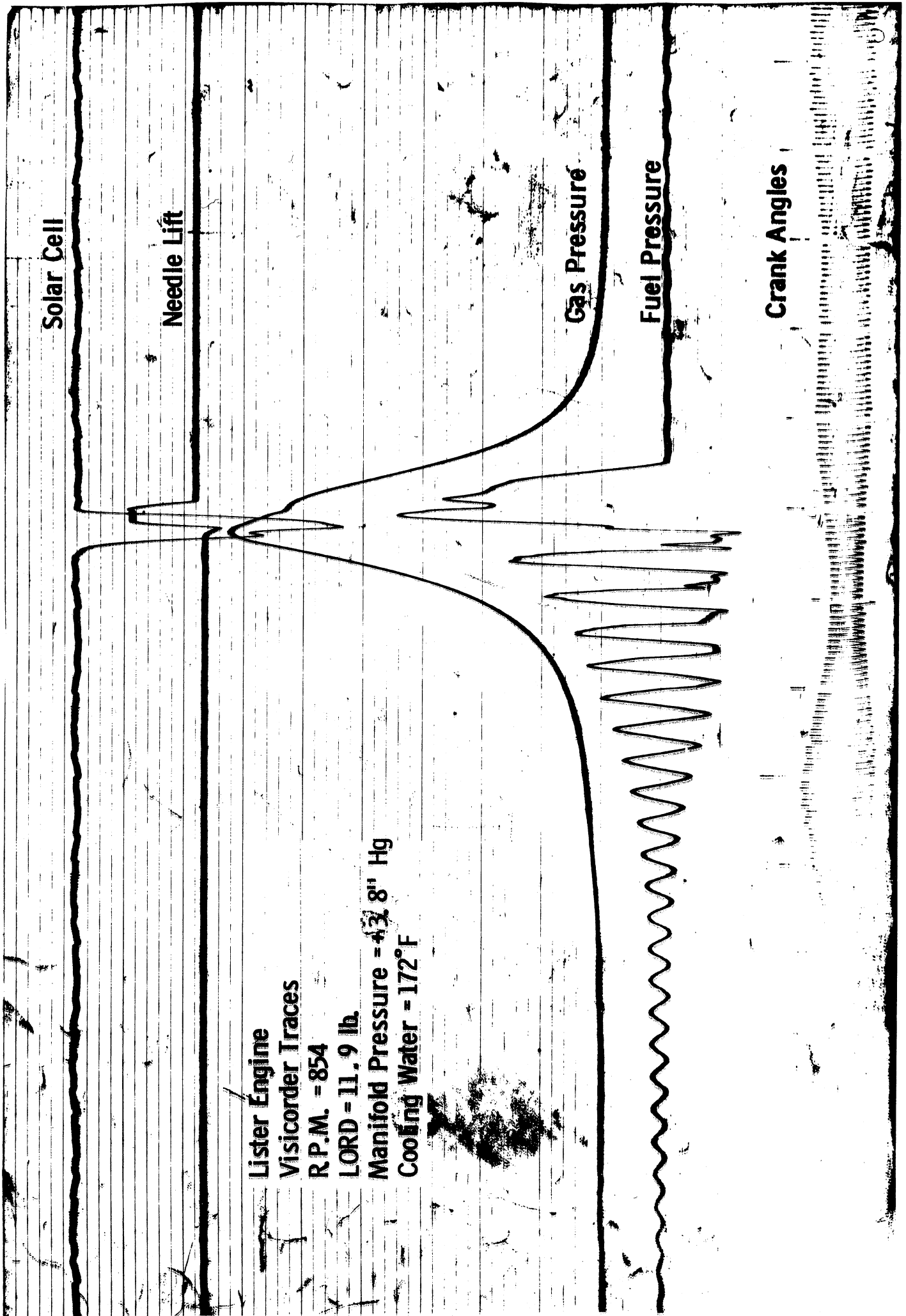


Figure 23. Visicorder traces.

APPENDIX II

TEST CONDITIONS AND RESULTS

TEST CONDITIONS

Barometric pressure = 30" Hg
Gauge pressure in inlet surge tank = 0
Gauge pressure before flowmeter = 85.5 psi
Air temperature before flowmeter = 71°F
Air temperature in inlet manifold = 102°F
Cooling water temperature at inlet = 162°F
Cooling water temperature at exit = 174°F
Exhaust gas temperature = 495°F
Average time for consumption of 0.12655 lb of fuel = 4.32 min
(fuel leakage from injector = 23.5 cm³/hr
Brake load = 16
Revolutions per minute = 1000 rpm

RESULTS

Air flow rate = 74.2 lb/hr
Fuel flow rate = 1.714 lb/hr
Fuel-air ratio = 0.0231
Brake horsepower = 2.67
B.M.E.P. = 30.4 psi
B.S.F.C. = 0.645 lb/B.H.P., hr

APPENDIX III

HEAT RELEASE

According to the first law of thermodynamics

$$\begin{aligned}
 dQ &= dU + dW \\
 &= m c_v dT + p \frac{dV}{J} \\
 \frac{dQ}{d\theta} &= m c_v \frac{dT}{d\theta} + \frac{p}{J} \frac{dV}{d\theta}
 \end{aligned} \tag{13}$$

From the equation of state

$$\frac{dT}{d\theta} = \frac{1}{mR} \left(p \frac{dV}{d\theta} + v \frac{dP}{d\theta} \right)$$

Substituting in equation (13) we get

$$\begin{aligned}
 \frac{dQ}{d\theta} &= \frac{c_v}{R} \left(p \frac{dV}{d\theta} + v \frac{dP}{d\theta} \right) + \frac{p}{J} \frac{dV}{d\theta} \\
 &= \left[\left(\frac{c_v}{R} + \frac{1}{J} \right) p \frac{dV}{d\theta} + \left(\frac{c_v}{R} \right) v \frac{dP}{d\theta} \right]
 \end{aligned} \tag{14}$$

BIBLIOGRAPHY

1. Alcock, J. F., "Air Swirl in Oil Engines," Proc. I.M.E. (London), Vol. 128, 1934, pp. 123-193.
2. Bolt, Jay A., and Henein, N. A., "Diesel Engine Ignition and Combustion," 06720-3-P report. The University of Michigan, Dec. 1965.
3. Bauer, S. G., "Ignition Lag in Compression Ignition Engines," Engineering, Vol. 148, p. 368, 9 (1939).
4. Heldt, P. M., "High-Speed Diesel Engines," 7th ed., Nyack, N. Y., 1953, p. 117.
5. Keenan, J. H. and Kaye, J., "Gas Tables," New York: John Wiley and Sons Inc., 1950.
6. Rosen, C. G. A., "Matching Fuels to Diesel Combustion Systems," SAE Trans. Vol. 71, 1963, pp. 259-271.
7. Tsao, K. C., Myers, P. S. and Uyehara, O. A., "Gas Temperature During Compression in Motored and Fired Diesel Engines," SAE Trans., Vol. 70, 1962, pp. 136-145.
8. West, A. C. and Taylor, Denis, "Ignition Lag in a Supercharged Compression-Ignition Engine," Engineering, April 11, 1941, p. 281 and 282.
9. Wolfer, H. H., "Ignition Lag in the Diesel Engine (Der Zundverzug im Dieselmotor), V.D.I. Forschungsheft No. 392, 1938, pp. 15-24, English translation-RAE report. _____.

UNIVERSITY OF MICHIGAN



3 9015 02229 1309